PB85-122414

Electrical Resistivity Technique to Assess the Integrity of Geomembrane Liners

Southwest Research Inst., San Antonio, TX

Prepared for

Municipal Environmental Research Lab.
Cincinnati, OH

Nov 84

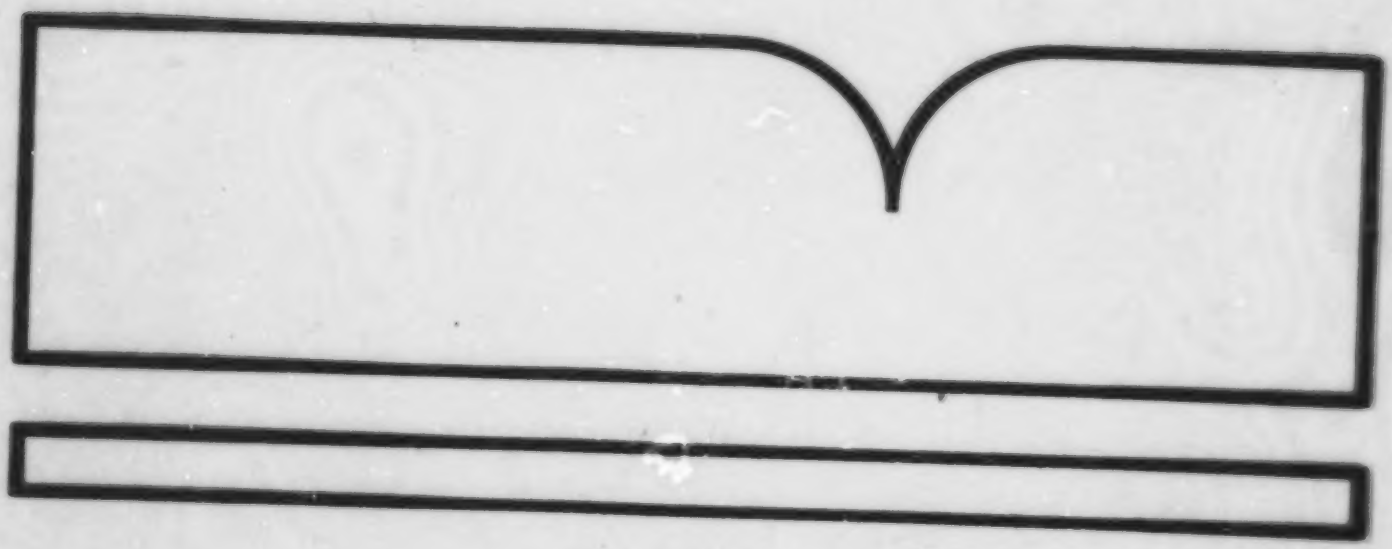

U.S. Department of Commerce
National Technical Information Service
NTIS

PB85-122414

EPA-600/2-84-180
November 1984

ELECTRICAL RESISTIVITY TECHNIQUE TO ASSESS THE INTEGRITY OF GEOMEMBRANE LINERS

by

David W. Shultz
Bob M. Duff
Wendell R. Peters
Southwest Research Institute
San Antonio, Texas 78284

Contract No. 68-03-3033

Project Officer

Carlton C. Wiles
Solid and Hazardous Waste Research Division
Municipal Environmental Research Laboratory
Cincinnati, Ohio 45268

MUNICIPAL ENVIRONMENTAL RESEARCH LABORATORY
OFFICE OF RESEARCH AND DEVELOPMENT
U.S. ENVIRONMENTAL PROTECTION AGENCY
CINCINNATI, OHIO 45268

REPRODUCED BY
NATIONAL TECHNICAL
INFORMATION SERVICE
U.S. DEPARTMENT OF COMMERCE
SPRINGFIELD, VA. 22161

TECHNICAL REPORT DATA
(Please read Instructions on the reverse before completing)

1. REPORT NO.	2.	3. RECIPIENT'S ACCESSION NO.
EPA-600/2-84-180		PB85 122414

4. TITLE AND SUBTITLE
Electrical Resistivity Technique to Assess the Integrity of Geomembrane Liners

5. REPORT DATE
November 1984

6. PERFORMING ORGANIZATION CODE

7. AUTHOR(S)
David W. Shultz
Wendell R. Peters
Robert M. Duff, Ph.D.

8. PERFORMING ORGANIZATION REPORT NO.

9. PERFORMING ORGANIZATION NAME AND ADDRESS
Southwest Research Institute
P.O. Box Drawer 28510
6220 Culebra Road
San Antonio, Texas 78284

10. PROGRAM ELEMENT NO.
BRD1A

11. CONTRACT/GRANT NO.
68-03-3033

12. SPONSORING AGENCY NAME AND ADDRESS
Municipal Environmental Research Laboratory--Cin.,OH
Office of Research and Development
U.S. Environmental Protection Agency
Cincinnati, Ohio 45268

13. TYPE OF REPORT AND PERIOD COVERED
Final - Sept. 1980-July 1984

14. SPONSORING AGENCY CODE
EPA/600/14

15. SUPPLEMENTARY NOTES
Carlton C. Wiles, Project Officer - 513/684-7795

16. ABSTRACT

Two-dimensional electrical modeling of a liner system was performed using computer techniques. The modeling effort examined the voltage distributions in cross sections of lined facilities with different leak locations. Results confirmed that leaks in the liner influenced voltage distributions on the surface of the lined facility.

Based on this, a small physical scale model of a lined facility was constructed. Tests were conducted to measure the influence of leaks on the surface voltage distributions of water-filled and earth-filled liner systems. Several leak and current electrode configurations were examined. Plots of measured surface voltages indicated the presence and location of a leak. These tests verified that the electrical resistivity technique could be used for detecting and locating leaks in liners.

Larger-scale testing was performed at a 1-acre lined water impoundment. An experimental measurement system was designed and constructed to facilitate data acquisition for various leak locations, water depths, and leak sizes. These data showed the technique to be capable of detecting a 1-inch diameter hole in the liner with an error in location of potentially less than 1 foot.

17. KEY WORDS AND DOCUMENT ANALYSIS

a. DESCRIPTORS	b. IDENTIFIERS/OPEN ENDED TERMS	c. COSATI Field/Group
		99

18. DISTRIBUTION STATEMENT	19. SECURITY CLASS (This Report)	21. NO. OF PAGES
Release to Public	Unclassified	78
	20. SECURITY CLASS (This page)	22. PRICE
	Unclassified	

EPA Form 2220-1 (Rev. 4-77) PREVIOUS EDITION IS OBSOLETE

DISCLAIMER

The information in this document has been funded wholly or in part by the United States Environmental Protection Agency under Contract No. 68-03-3033 to Southwest Research Institute. It has been subject to the Agency's peer and administrative review, and it has been approved for publication as an EPA document. Mention of trade names or commercial products does not constitute endorsement or recommendation for use.

FOREWORD

The U.S. Environmental Protection Agency was created because of increasing public and government concern about the dangers of pollution to the health and welfare of the American people. Noxious air, foul water, and spoiled land are tragic testimonies to the deterioration of our natural environment. The complexity of that environment and the interplay of its components require a concentrated and integrated attack on the problem.

Research and development is that necessary first step in problem solution, and it involves defining the problem, measuring its impact, and searching for solutions. The Municipal Environmental Research Laboratory develops new and improved technology and systems to prevent, treat, and manage wastewater and solid and hazardous waste pollutant discharges from municipal and community sources, to preserve and treat public drinking water supplies, and to minimize the adverse economic social, health, and aesthetic effects of pollution. This publication is one of the products of that research and is a most vital communications link between the researcher and the user community.

This report documents the development and demonstration of an electrical resistivity technique to assess the physical integrity of geomembrane liners. The technique works by detecting and locating potential fluid leak paths in the liner. The developmental procedures implemented to create and test this technique are described and test results are presented.

Francis T. Mayo
Director
Municipal Environmental Research
Laboratory

PREFACE

Geomembrane liners (often called flexible membrane liners) are sheets of plastic or rubber materials used to contain fluids, most often in earthen structures. Facilities where these liners are commonly used include water reservoirs, landfills, and surface impoundments. At certain types of facilities, it is important to know whether the liner is intact and performing its intended containment function. Examples are hazardous waste landfills and fluid impoundments. Loss of fluid from these facilities may create groundwater and surface water contamination. Geomembrane liners are inspected to various degrees for physical integrity during installation. Visual inspection combined with seam testing is typical. However, no method has been available to test the entire geomembrane liner system. Such testing is desirable because repairs could easily be made before placing the liner into service. Efforts to monitor the performance of liners have typically relied on groundwater sampling around the facility as an indirect indication of leakage. This method is not precise enough for monitoring liner performance, since groundwater contamination may take years to occur. In addition, monitoring wells may never detect contamination if they are not located in the contaminated groundwater aquifer.

Recognizing the need for a method to detect and locate leaks in geomembrane liners, the U.S. Environmental Protection Agency intitiated a program to develop and demonstrate several techniques or techniques to detect and locate leaks in geomembrane liners. The techniques included time domain reflectometry, acoustic emission monitoring, and electrical resistivity. This report presents the results of the project conducted to develop and demonstrate the electrical resistivity technique.

ABSTRACT

This report documents a surface electrical resistivity technique to detect and locate leaks in geomembrane liners. These materials exhibit resistance to the flow of electrical current. Thus a fluid path through the geomembrane will form a detectable electric current path by which a leak may be detected and located.

Two-dimensional electrical modeling of a liner system was performed using computer techniques. The purpose of this modeling effort was to examine the voltage distributions in cross sections of lined facilities with different leak locations. Results confirmed that leaks in the liner influenced voltage distributions on the surface of the lined facility.

Based on these results, a small, three-dimensional, outdoor, physical scale model of a lined facility was designed and constructed. Tests were conducted to measure the influence of leak paths on the surface voltage distributions of both water-filled and earth-filled liner systems. Several leak and current electrode configurations were examined. Contour plots of measured surface voltages indicated the presence and location of a leak. These model tests verified that the electrical resistivity technique could be used for detecting and locating leak paths in liners. Large testing of the technique was necessary for further defining performance and developing measurement and data analysis procedures.

This large-scale testing was performed at a 1-acre lined water impoundment located at Southwest Research Institute. An experimental measurement system was designed and constructed to facilitate data acquisition for various leak locations, water depths, and leak sizes. These data showed the technique to be exceptionally well suited to the application and capable of detecting a 1-inch diameter hole in the liner with an error in location of less than 1 foot.

This report was submitted in fulfillment of Contract No. 68-03-3033 by Southwest Research Institute under the sponsorship of the U.S. Environmental Protection Agency. This report covers the period September 1980 to July 1984, and work was completed as of November 1983.

CONTENTS

Foreword iii
Abstract v
Figures. viii
Abbreviations and Metric Conversion Table. xi
Acknowledgments. xii

1. Introduction 1
2. Conclusions 2
3. Recommendations 6
4. Research Approach 8
    Background. 8
    Concept Development 9
    Large-Scale Testing 34
5. Results and Discussion. 53
    Overview. 53
    No-Leak Survey Results. 53
    Simulated Leak Survey Results 60
    Seam Leak Simulation Results. 69
    Summary of Large-Scale Testing. 75

References 77

FIGURES

Number		Page
1	Conceptual electrical resistivity testing technique applied to detect and locate leaks in a geomembrane liner system	11
2	Two-dimensional computer model of a liner having no penetration leaks but with an electrical current path over the upper edges.	19
3	A rectilinear array network (partially shown) of 21 x 11 resistors used to model a geomembrane liner.	19
4	Two-dimensional computer model of a liner with a leak.	20
5	Two-dimensional computer model of a liner with a leak at the bottom of the berm	20
6	Instrumentation used to conduct physical scale model tests	23
7	Block diagram of instrumentation used to conduct model tests	24
8	Physical scale model showing the plastic liner and shunt resistors.	25
9	Potential measurements being taken using the fiberglass beam which supports electrodes.	25
10	Equipotential plot of voltages on the surface of the water with a single leak	28
11	Equipotential plot of voltages on the surface of the water with a highly conductive aluminum block and one leak	28
12	Equipotential plot of voltages on the surface of the water with a single leak near the edge of the liner.	30
13	Equipotential plot of voltages on the surface of the water with two leaks 20° apart	30
14	Equipotential plot of voltages on the surface of the water with two leaks 40° apart	30
15	Equipotential plot of voltages on the surface of the water with a single leak	31

FIGURES (Continued)

Number		Page
16	Equipotential plot of voltages on the surface of the soil with a single leak	31
17	Equipotential plot of voltages on the surface of the soil with a single leak	33
18	Equipotential plot of voltages on the surface of the soil with two leaks 40° apart	33
19	Plan view of the test impoundment.	35
20	Cross section A-A' of the test impoundment	35
21	Test impoundment construction activity	36
22	Liner installation activities.	37
23	Installation of a pipe designed as one of five leaks through the liner.	38
24	Rings used to hold plastic inserts designed to serve as leaks	40
25	Simplified block diagram of the equipment used to test the electrical resistivity technique	41
26	A mobile laboratory trailer, shown at the upper right, is used to house the instrumentation during testing.	43
27	Testing instrumentation inside the mobile laboratory	44
28	The electrically operated logging winch used during testing to control the location of the measurement electrode.	46
29	The circular brass disc below the end of the platform is used as the current source electrode during testing	47
30	The reference electrode and preamplifier housing are shown to the left of the potential measurement electrode box.	49
31	Conceptual drawing of the test impoundment and operation of the test equipment	50
32	A plot of the potential measurements taken along the 90° radial for a no-leak case.	54
33	An equipotential contour plot of no-leak measurements.	54

FIGURES (Continued)

Number		Page
34	A plot of the potential measurements taken along the 90° radial. .	56
35	An equipotential contour plot showing the distortions from a 1-foot diameter leak on the 90° radial	56
36	A plot of the potential measurements taken along the 90° radial. .	58
37	An equipotential contour plot showing the distortions from a 1-inch diameter leak	58
38	A plot of the potential measurements taken along the 115° radial .	60
39	An equipotential contour plot showing the distortions from a 1-foot diameter leak	60
40	A plot of the potential measurements taken along the 90° radial. .	61
41	An equipotential contour plot showing the distortions from a 1-foot diameter leak	61
42	A plot of the potential measurements taken along the 90° radial. .	63
43	An equipotential contour plot showing the distortions from a 1-foot diameter simulated leak	63
44	A plot of the potential measurements taken along the 90° radial. .	64
45	An equipotential contour plot showing the distortions from a 1-foot square simulated leak in 5 feet of water.	64
46	A plot of the potential measurements taken along the 90° radial. .	65
47	An equipotential contour plot showing the distortions from a 1-foot square simulated leak in 6.5 feet of water.	65
48	A plot of the potential measurements taken along the 90° radial. .	67
49	An equipotential contour plot showing the distortions from a 0.1-foot square simulated leak without metal cans.	67
50	A plot of the potential measurements taken along the 90° radial. .	68
51	An equipotential contour plot showing the distortions from a 0.1-foot square simulated leak with metal cans surrounding the leak	68
52	A plot of the potential measurements taken along the 90° radial. .	70

FIGURES (Continued)

Number		Page
53	An equipotential contour plot showing the distortions from a 0.4-foot square, 30-foot long wire used to simulate a seam leak	70
54	Plots of measurements along the 90° and 110° radials	72
55	An equipotential contour plot showing the distortions from two 1-inch diameter leaks on two different radials	72
56	Plots of measurements along the 90°, 110° and 115° radials	73
57	An equipotential contour plot showing the distortions from three 1-foot diameter leaks on three different radials	73
58	A plot of measurements along the 90° radial	74
59	An equipotential contour plot showing the distortions from three different sized leaks along the 90° radial	74

TABLES

Number		Page
1	Electrical Properties of Selected Geomembrane Liner Materials	10

LIST OF ABBREVIATIONS

EPA -- Environmental Protection Agency

FML -- flexible membrane liner

mil -- one thousandth of an inch

Hz -- hertz

AC -- alternating current

HDPE -- high-density polyethylene

dB -- decibel

DC -- direct current

FACTORS FOR CONVERTING DATA IN U.S. CUSTOMARY UNITS TO SI METRIC UNITS

inches to centimeters (cm)	x 2.54
feet to meters (m)	x 0.3048
mils to centimeters (cm)	x 2.54×10^{-3}
mils to millimeters (mm)	x 2.54×10^{-2}
acres to hectares (ha)	x 0.4

ACKNOWLEDGMENTS

This report was prepared by the Department of Geosciences, Southwest Research Institute. The authors wish to express appreciation to Carlton C. Wiles, whose valuable assistance as Project Officer helped guide this project to a successful completion.

The following persons were responsible for writing and editing major portions of the text:

David W. Shultz
Wendell R. Peters
Bob M. Duff
Thomas E. Owen

The following persons were responsible for field data collection and analyses:

Bob M. Duff
David W. Shultz
Frank X. Herzig
Kay Kuester
John Goodwin
Cliff Gulley

SECTION 1

INTRODUCTION

The United States generates large quantities of solid and hazardous industrial and municipal wastes each year. The U.S. Environmental Protection Agency (EPA) estimates that the annual production of hazardous wastes exceeds 57 million metric tons. This amount represents approximately 15 percent of all industrial wastes (Hanrahan, 1979; EPA, 1980).

The most common method of disposal of these wastes is on land. Land disposal includes landfills, surface impoundments, and land treatment. A nationwide survey reports there are 12,627 active landfills and 180,973 active surface impoundments in the United States (Surface Impoundment Assessment National Report, 1983). Fluids produced by landfills (leachates) or contained in surface impoundments are frequently toxic and contain substances that could cause contamination if released into nearby surface or groundwater resources.

To prevent contamination, geomembrane liner systems are often installed. Placing these liners beneath the landfill or surface impoundments creates a barrier that prevents or greatly inhibits migration of contaminating liquids. Geomembrane liners made of plastic or rubber are useful because of their low permeability. Geomembrane liners, often termed flexible membrane liners (FML's), are sheets of polymeric materials fabricated in a factory and seamed together at the field site to create a continuous liner system. Installation practices as well as operational factors can lead to punctures or separated seams, causing loss of physical integrity. Physical damage can also result from exposure to incompatible waste fluids.

Since the goal of geomembrane liner systems is only achieved when the liner retains its physical integrity, initial inspection and in-service testing of the physical integrity is important. In 1980, the U.S. Environmental Protection Agency initiated a research project to develop a liner physical integrity assessment technique. This effort has resulted in the development and demonstration of an electrical resistivity technique to determine liner integrity. The technique detects and locates areas of the liner system where physical integrity has been breached by the passage of a conducting liquid. The technique takes advantage of the high electrical insulating properties of the liner compared with the waste contained above the liner and the soil under the liner. If the liner is physically punctured or separated, the electrical conductivity of the fluid and underlying soil form a current path by which the leak may be detected and located. The technique can be applied on the surface of an existing landfill or fluid impoundment and will not damage the liner. It can be used to test new geomembrane liner systems before they are put into service. The technique incorporates digital data acquisition equipment,

which eliminates human errors in manual reading and recording of measured data, and it is portable to facilitate onsite application by two or three field personnel.

Southwest Research Institute developed and demonstrated the electrical resistivity liner assessment technique in three phases. The first phase involved formulation of mathematical concepts and the computer modeling of a liner system. Two-dimensional models were used to examine the electrical current distribution in the cross sections of simulated landfills or surface impoundments having electrically resistive geomembrane liner systems in place. Results of the conceptual development and computer model studies demonstrated the soundness of the electrical resistivity technique. The second phase involved the construction of a small 10- by 10-foot three-dimensional physical scale model using a geomembrane in a wooden frame. Results of the physical scale model tests demonstrated that the electrical resistivity technique could be used to detect and locate leaks in a geomembrane liner for both soil-filled and water-filled test conditions. Based on these investigative studies, the hardware needed to test the technique under large-scale conditions was designed and assembled for testing in the third phase of the work. These large-scale tests were performed in a 0.4-ha (1-acre) geomembrane-lined facility at Southwest Research Institute.

SECTION 2

CONCLUSIONS

A surface electrical resistivity technique to examine the physical integrity of a geomembrane liner system has been developed and demonstrated. The technique performs by detecting and locating electrical current paths through a geomembrane. The technique has excellent potential for meeting industry needs for testing liners installed in hazardous solid waste and surface impoundments. The technique can also be used to inspect liner integrity immediately after installation at new facilities, and to inspect in-service geomembranes without interruption of facility use.

Conclusions regarding the technique are:

(1) A geomembrane liner survey using the technique will not damage the liner.

(2) The instrumentation and hardware required to apply the technique are portable.

(3) The technique has been performance tested at a 1-acre, water-filled, polyethylene-lined test impoundment. The technique has detected a 1-inch-diameter leak path in the liner and located it to within 1 foot of the actual location in 5 feet of water. Similar results have been obtained for multiple leak path configurations and tests in water depths of 6.5 feet.

(4) The results of scale-model testing with soil fill suggest that a the system may be used to survey liners installed at existing landfills.

(5) The results of experiments designed to determine the influence of the depth of water on the measurements suggest that increasing depth may reduce the magnitude of the measurements.

(6) The results of experiments designed to measure the effect of highly conductive metal objects located close to a leak path indicate that the performance of the technique is not significantly influenced by the presence of the objects.

(7) The results of an experiment simulating a seam leak in the liner indicate that the geometry of a leak may influence the measurements obtained on the surface of the water.

SECTION 3

RECOMMENDATIONS

Based on the results of this project, the following recommendations are made regarding the electrical resistivity technique:

(1) Evaluate the electrical resistivity technique at lined surface impoundments and landfills where design and liner integrity status information is available or can be experimentally determined. It would be desirable to conduct the first test at a fluid impoundment to allow comparison of the results with the tests performed at the 1-acre test impoundment.

(2) Use the technique to test the integrity of an installed liner before that liner is placed in service. This would allow immediate verification of the test results, since access to any part of the liner would be possible.

(3) Determine the applicability of the technique for testing other types of liner materials such as asphalt, sprayed-on membranes, soil cement, clays, concrete, and soil sealants.

(4) Determine the applicability of the technique for testing double liner systems (i.e., those in which two membrane liners are installed with a drain layer between the liners).

(5) Specify the modifications to existing equipment, instrumentation and survey procedures that would be necessary to test liners at hazardous waste impoundments or landfill sites.

(6) Continue the development of a computer model to predict the response of liner systems to electrical resistivity testing, given facility design information such as geometry, liner type, waste type, surface area, and depth of waste.

(7) Continue to develop computer analyses of liner survey results to enhance the determination of leak signatures.

(8) Define and evaluate liner design and installation techniques that would enhance the applicability and usefulness of the electrical resistivity testing technique.

(9) Evaluate the applicability of the electrical resistivity survey technique for continuous automatic monitoring of geomembrane liner systems.

SECTION 4

RESEARCH APPROACH

BACKGROUND

Liners are installed in hazardous waste treatment and disposal facilities such as landfills and surface impoundments to impede the flow of contaminating fluids into surface and groundwater resources. Since liners made from polymeric materials such as plastics and rubbers have very low water permeabilities, they are effective fluid containment membranes.

If the liner fails to provide physical integrity, then the liner cannot function as intended. Tears, ruptures, imperfect seam joints, or areal degradation would allow fluid to penetrate into the underlying soil, violating the intent of the liner. Thus if a technique were available to test the liner during installation before facility startup, during the operation of the facility, and after the facility is closed, the goals of water resource protection would be better served.

Ideally, the testing method should be appropriate for assessing a broad range of liner materials. It should be inexpensive, portable, and suitable for inspecting liners installed in any type of facility. The technique should not require burial of sensing elements below the liner, since this would not allow inspection of existing liner installations. The method must not only be capable of detecting the presence of a leak, but also of locating the leak so that appropriate remedial measures can be implemented. The method must operate without damage to the liner.

In 1980, Southwest Research Institute initiated a project funded by the U.S. Environmental Protection Agency to evaluate a surface electrical resistivity technique applicable to these inspection and monitoring requirements. This technique was based in part upon previous work performed by the Institute to develop a high-resolution earth resistivity method for detecting small subsurface cavities. When this project was initiated, no techniques were available to test the physical integrity of installed liners. In addition, no practical methods were available to test the entire liner system after installation but prior to facility startup. The remaining body of this report presents the research studies conducted to develop and demonstrate an electrical resistivity technique to meet the liner testing objectives.

CONCEPT DEVELOPMENT

Theoretical and Mathematical Formulation

Geomembrane liners made from impervious plastics and rubbers exhibit very high electrical resistance. When a liner is installed in a landfill or surface impoundment, it effectively acts as an electrical insulator between the materials contained in the facility and the surrounding earth. Electrical properties of selected geomembrane liner materials commonly used are presented in Table 1. If the liner is physically punctured or separated, conductive fluid flow through the leak establishes an electrical shunt through the liner. This low resistance shunt forms an electrically detectable region which is the basis by which a leak may be detected and located.

TABLE 1. ELECTRICAL PROPERTIES OF SELECTED GEOMEMBRANE LINER MATERIALS

Material Type	Thickness of Specimen (mils)	Area of Specimen (cm^2)	Electrical Resistance (ohms)	Volume Resistivity (ohm - cm)
High Density Polyethylene (A)	55.0	100.0	4.00×10^{13}	2.86×10^{16}
High Density Polyethylene (B)	121.0	45.5	3.25×10^{13}	4.81×10^{15}
Polyethylene	6.0	100.0	1.80×10^{11}	1.18×10^{15}
Chlorosulfonated Polyethylene (A)	40.0	100.0	3.20×10^{8}	3.14×10^{13}
Chlorosulfonated Polyethylene (B)	36.0	100.0	3.75×10^{10}	4.10×10^{13}
Chlorosulfonated Polyethylene - nylon reinforced	34.0	100.0	3.60×10^{9}	4.16×10^{12}
Polyvinyl Chloride	29.0	100.0	1.52×10^{8}	2.06×10^{11}
Polyvinyl Chloride - oil resistant	30.0	100.0	1.70×10^{8}	2.23×10^{11}
Chlorinated Polyethylene	32.5	9.0	7.20×10^{10}	7.84×10^{12}
chlorinated Polyethylene - reinforced	36.0	100.0	6.20×10^{8}	7.32×10^{11}
Urethane Asphalt	69.0	100.0	2.20×10^{11}	1.25×10^{14}

Source: Laboratory tests performed by SwRI.

Figure 1 shows the basic surface electrical resistivity testing technique for detecting and locating a leak in a geomembrane liner. A current source is used to inject current across the boundary of the liner. The liner has an electrical leak path, as shown. When a voltage is applied between the source and remote current return electrodes, current flows through the leak as shown in the figure. If a soil cover were present over the edges of the liner, current would also flow through this soil cover to the remote current return electrode, bypassing the liner. Potentials measured on the surface are affected by the current distributions near the leak and can be used to locate the leak.

The success of the electrical resistivity technique in detecting leaks depends upon the liner material having a high resistance per unit area compared with that of a leak path. The current flow lines shown in Figure 1 for a liner having a leak assume an essentially perfect insulator for the liner material. If the liner were a perfect insulator and there were no current conducting paths through leaks over the top of the liner, no current would flow. However, geomembrane liner materials have a high but finite resistivity. Therefore, some current will penetrate the liner under any conditions. If the current density through the liner is assumed to be uniform, then the total resistance which the liner presents as a load across the source can be computed from the formula:

$$R_L = \frac{\rho_L t}{A} \qquad (1)$$

where:

R_L = the total liner resistance (ohms);
ρ_L = the volume resistivity of the liner material (ohmmeters);
t = the thickness of the liner (meters); and
A = the total surface area of the liner (square meters).

For a liner 7.62×10^{-4}m (30 mils) thick and 2.01×10^{4}m^2 (five acres) in area consisting of a material having a volume resistivity of 2×10^{10} ohmmeters, Equation (1) gives a total liner resistance of 750 ohms. Thus, even though the resistivity of the liner material is high, the total circuit resistance caused by the insulating liner can be relatively small for a large facility. For practical liner materials, the location of the current electrode within the lined landfill or impoundment and the shape of the containment area will result in a nonunifrom current density through the liner even for the no-leak case. Equation (1) must therefore be considered as a first approximation to the total resistance of the liner. Nevertheless, it is useful for estimating performance of the technique.

The total electrical resistance load across a direct current source connected between the source current electrode inside of the impoundment region and a remote current return electrode located at effective infinity outside of the impoundment will consist of the series combination of a resistance, R_F, of the fill inside of the liner, the resistance, R_L, of the liner and shunting leak paths, and a resistance, R_E, of the earth surrounding the impoundment.

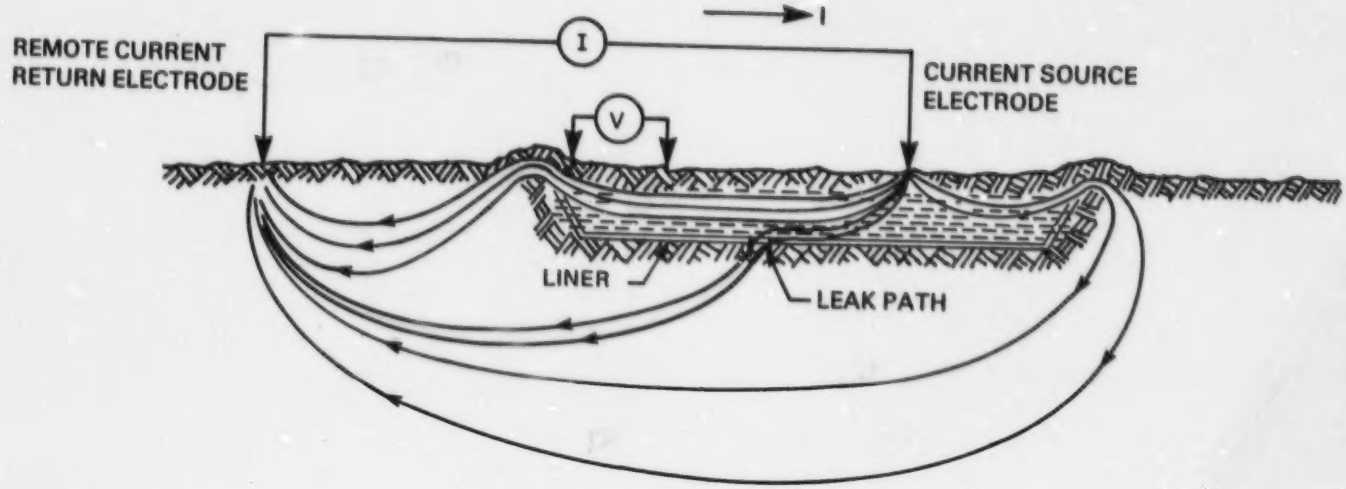

Figure 1. Conceptual electrical resistivity testing technique applied to detect and locate leaks in a geomembrane liner system.

Each of these resistances is dependent upon the volume resistivity of the medium and the geometry of the installation. The resistance, R_L, is the parallel combination of the resistance across the liner material and the resistance of any conducting leak paths. If an alternating current source is used, the liner will exhibit a capacitive reactance in parallel with the total resistance described above. At a large liner site, this capacitance can be significant and its reactance even at frequencies as low as 10 Hz may be comparable to the resistance of the liner. This capacitive impedance of the liner is primarily of importance in the design of the current source system rather than in the interpretation of the measurements.

A mathematical model capable of predicting the potential at the surface of an impoundment as a function of leak size and location will be beneficial in evaluating electrical restivity technique performance, as well as aiding the interpretation of measurements. The field equations which must be solved for the direct current case are:

$$\nabla \cdot E = q_f/\varepsilon_o \tag{2}$$

$$\nabla \times E = 0 \tag{3}$$

$$\nabla \cdot J = 0 \tag{4}$$

where:

E = electric field intensity;
J = volume density of electric current;
q_f = volume density of free charge; and
ε_o = permittivity of free space (8.854×10^{-12} farads/meter).

Equation (3) allows the electric field to be expressed in terms of a scalar potential function, ϕ, as

$$E = -\nabla\phi \tag{5}$$

Combining Equations (5) and (2) results in the familiar Poisson's equation of potential theory

$$\nabla^2\phi = -q_f/\varepsilon_o \tag{6}$$

Since free charge can exist only at the source and on surfaces of discontinuity, Equation (6) reduces to Laplace's equation everywhere within the regions of interest

$$\nabla^2\phi = 0 \tag{7}$$

Equations (2) through (7) are strictly valid only for the direct current case. When a low frequency alternating current is used, a quasistatic form of Maxwell's equations would be more accurate. Since the frequency used for the measurements is 17 Hz, even for the largest impoundments this change only requires that Equation (4) be replaced by

$$\nabla \cdot J = -j\omega q_f \tag{8}$$

where ω = angular frequency of the current. This modification includes the capacitive impedance effect of the liner.

A useful understanding of the problem can be obtained from an examination of the boundary integral equation:

$$\phi(r) = \frac{I\rho_1}{2\pi r} - \int_{S_L} \phi(r') \frac{\partial}{\partial n} \frac{1}{R} \, da' - \rho_1 \int_{S_L} \frac{J_n(R')}{R} \, da' \tag{9}$$

where:

r = the distance from the current injection electrode (inside the facility) to the point on the surface at which the potential is measured;

$\phi(r)$ = the potential at point r on the surface;

I = the total injected current;

r' = the distance from the current injection electrode to the point of integration on the liner;

R = the distance between the potential measuring point r and the integration point r';

$J_n(r)$ = the component of current density perpendicular to the surface of integration, i.e., liner;

S_L = the surface S_L with leak areas removed;

ρ_1 = the volume resistivity of material within the facility, i.e., liquid or solid waste; and

n = a unit vector normal to the surface S_L.

The integrations in Equation (9) are surface integrals over a surface defined by the liner and leak areas. The potential $\phi(r)$ on the liner surface can be shown to be directly related to the current density crossing the surface. Thus, both integrals in Equation (9) are dependent on the distribution of current and the resulting potential at the surface is determined by this current distribution. While the total resistance of the liner at a large site may be small, the resistance per unit area of liner material is still very high compared with a leak. The current density at a leak will therefore be many times as great as that at any point on the liner. A leak may then be expected to have a strong effect on the localized potential measured at the surface of the impoundment.

A second feature which may be observed in Equation (9) is that the integrands on the right-hand side of the equation are inversely related to the

distance between the measurement point and the integration point on the liner surface. The greatest perturbation of the surface potential by a leak will therefore occur directly over the leak. The conclusions which may be drawn from Equation (9) are that the high current density flowing through a leak will be detected from potential measurements on the surface and that the distribution of potential on the surface will indicate the location of the leak.

For prediction of system performance at large impoundment sites, the question of leak detectability as a function of depth of fill arises. An accurate answer to this question will require detailed numerical solution of the mathematical model. However, an approximate analysis of this problem can be obtained from examination of scaling laws. In other words, rather than attempting to vary only the depth of a given site, consider sites of similar geometry but different overall dimensions. For leaks which are not too close to the edges of the liner this analysis should provide a reasonable prediction of the dependence of potential distribution on the depth of fill.

If all length dimensions, L, are changed by a factor n so that,

$$L_n = nL \tag{10}$$

where:

L = the original length unit; and
L_n = the scaled length unit;

then, from examination of Equation (9) or other basic equations it can be shown that

$$\phi_n(r) = \frac{1}{n}\,\phi(nr) \tag{11}$$

Since this relationship is based on a scaling of all dimensions, the thickness of the liner and size of the leak are scaled by the same factor as the depth. The multiplicative factor 1/n may be expected to be significantly changed if one liner thickness is retained. The distribution of potential as given by Equation (11) is a good estimate. Thus, the measurements at two sites, one being n times as deep as the other and having a leak of n times the area, will be similar if the data from the deeper site is plotted with a 1/n change of length scale. For example, measurements collected for a one-inch diameter leak at a depth of 5 feet are expected to be similar to measurements for a 5-inch diameter leak at a depth of 25 feet.

Model studies were performed to validate the electrical resistivity liner survey technique. These studies provided an opportunity to experimentally analyze the current distribution and surface potentials resulting from various leak configurations. This information was needed to develop field survey equipment. The modeling studies and results are presented in the next section.

Computer Modeling Studies

Two-dimensional resistive network computer modeling studies were performed to predict the influence of an electrical current penetration through a geomembrane liner and associated surface potential voltages inside a landfill or fluid impoundment. The influences sought were the magnitude of the surface potentials at given locations for cases where fluid leaks or electrical current paths existed through the liner. The two-dimensional resistor network designed to simulate a liner was modeled using a general purpose circuit simulation computer program called SPICE. This software allows simulation of circuits containing resistors, capacitors, inductors, and voltage and current sources. The resistivity of the fill inside the liner (either soil or fluid) and the earth surrounding the liner was modeled using normalized resistance values of one ohm. The liner was characterized in the model by using parallel 1000-ohm resistors along the path of the liner. To simulate a leak or conductive path through the liner, one of the 1000-ohm resistors in the liner was replaced by a 1-ohm resistor. Therefore, the leak path has the same resistance as the earth. In effect, the liner is thus removed at that location.

A soil cover over a geomembrane liner will serve as an electrical conductive shunt for electrical current into the surrounding earth. This shunting effect was modeled by using 2-ohm resistors at the surface. It was included in the model since landfills and surface impoundments may have soil covers. A current source was used in the model to inject current into the surface of the earth as modeled in the program.

The output of the model analysis is the voltage at each of the nodes connecting the sensor elements. These values are stored in an array which is then used in a second program which plots the results in the form of equipotential contours. Figure 2 illustrates a contour plot showing the two-dimensional potential distribution around a liner without leaks. The current flow over the top of the liner into the surrounding earth is shown. The network used to model this cross section was a rectilinear array of 21 by 11 resistors, shown in part in Figure 3, for a total of 494 elements. The current injection point is at the top center of the figure with the other reference electrode connected to a conducting path along the bottom and sides of the cross section. This reference is far enough from the liner to be located at effective infinity.

Computer Results--

Figure 4 illustrates the results of one of the computer generated two-dimensional analyses of a liner having a leak in the bottom. The equipotential lines which appear in the figure are generated and plotted automatically by the computer program described earlier. The outline of the liner has been sketched in the figure and is represented by the three-sided trapezoidal figure in the center of the plots. The equipotential lines showing the voltage distribution patterns were computer generated. The current flow paths are at right angles to the equipotential lines and were sketched in by hand.

This figure shows that, as predicted, when a leak penetration is present in the liner, current flow between electrodes located inside and outside the

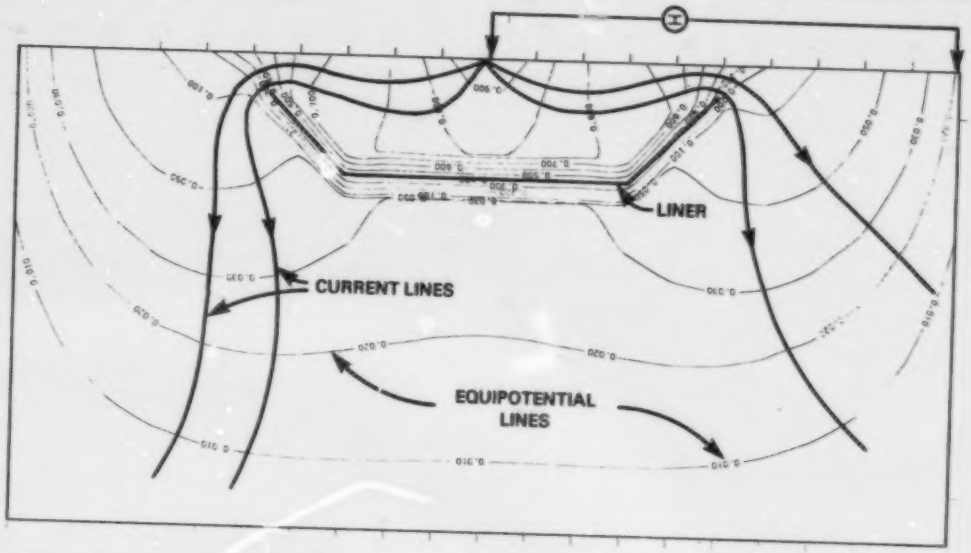

Figure 2. Two-dimensional computer model of a liner having no penetration leaks but with an electrical current path over the upper edges.

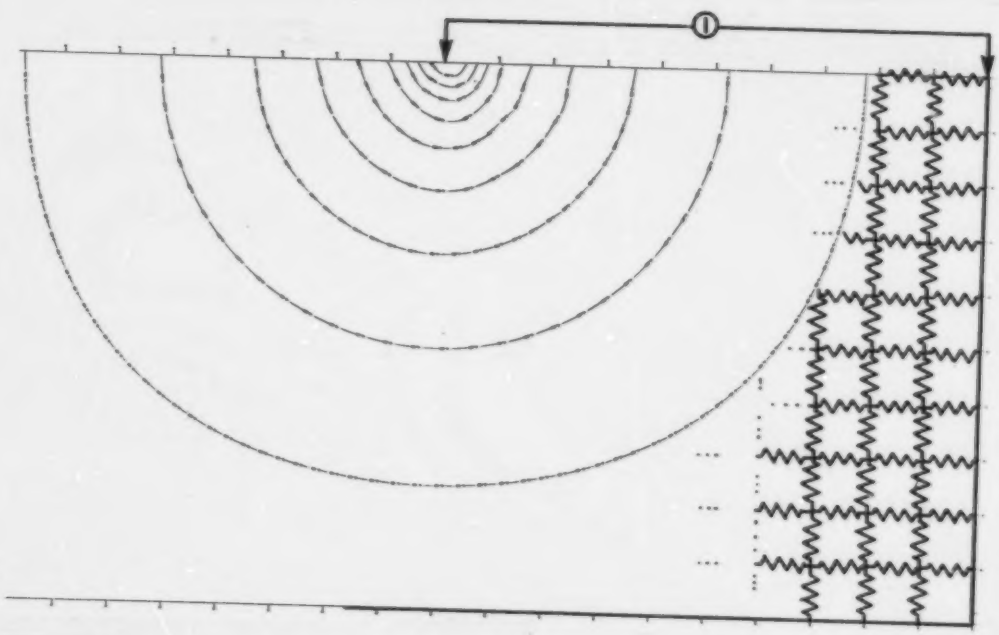

Figure 3. A rectilinear array network (partially shown) of 21 x 11 resistors used to model a geomembrane liner.

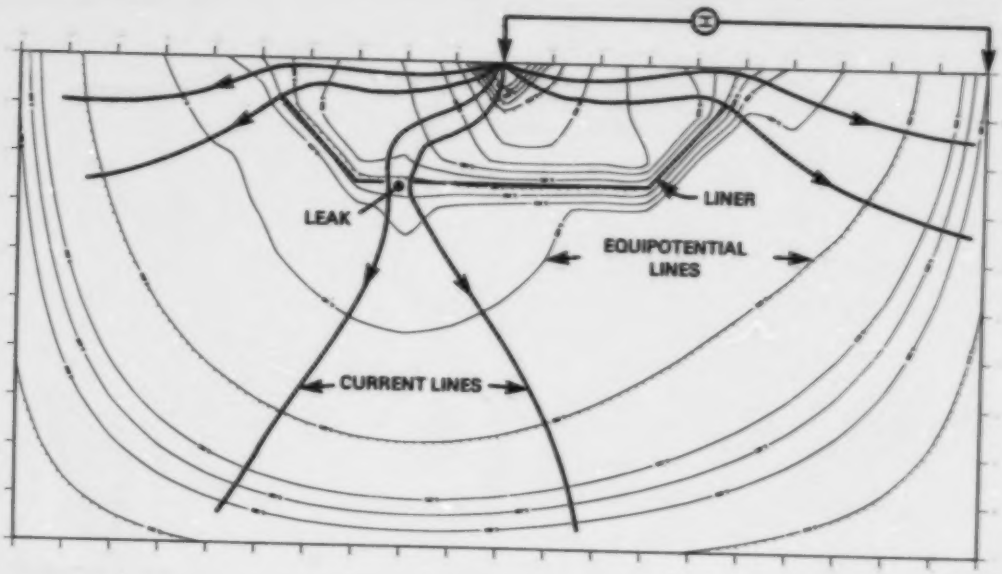

Figure 4. Two-dimensional computer model of a liner with a leak. Equipotential lines at the top are non-symmetrical, indicating the presence of a leak.

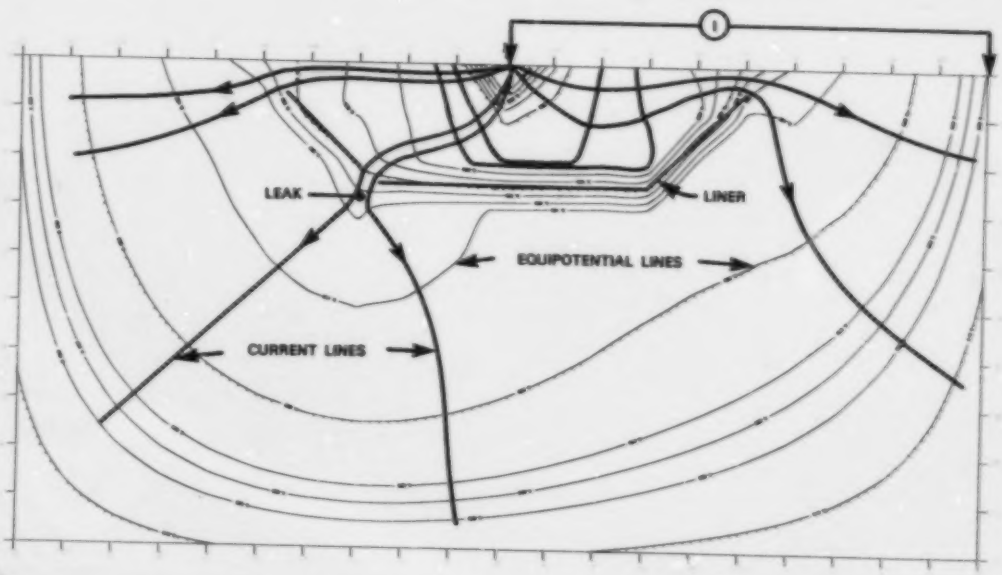

Figure 5. Two-dimensional computer model of a liner with a leak at the bottom of the berm.

liner will follow two paths, namely, through the leak and over the buried edges of the liner. Note the non-symmetry of the equipotential lines terminating on the surface of the facility, above the liner. The voltage gradient is clearly steeper along the surface on the left side of the current injection electrode above the leak.

Figure 5 shows the results of another computer generated two-dimensional analysis of a liner having a leak near the edge of the liner. The equipotential lines at the surface are influenced by the leak in a different manner than in the previous example. Thus, the location of the leak changes the relative distribution of voltages on the surface. It is this effect which was examined and investigated further to develop hardware and data reduction techniques to locate liner leaks.

The relatively inexpensive nature of the two-dimensional computer model and its precise control make it a very productive method of investigating electrical testing concepts related to liner leaks. Even though it is a two-dimensional model that does not accurately simulate the three-dimensional volume of a landfill or surface impoundment, the ability to accurately predict the potential distribution in various simulations of liner conditions makes it a valuable tool. The sensitivity of this model to a simulated leak is greater than for a true landfill condition because of the two-dimensional character of the model. Nevertheless, the results obtained are, in general, indicative of the full-scale equipment sensitivity requirements.

Based upon the results of the computer analyses, a three-dimensional physical scale model was designed and constructed. The following section describes the model and presents the experimental results.

Physical Scale Modeling Studies

After completion of the computer modeling studies, a three-dimensional physical scale model was designed and constructed. The objectives of using this model were to: (1) observe the surface voltage distribution patterns created by a fixed liner geometry, injection current location, fill material inside the liner, and leak configuration; (2) test the system instrumentation and assess its suitability for full scale testing; and (3) determine the accuracy of the technique in locating a leak.

Model Design--

The model was designed to allow studies of the resolution capabilities of the technique, i.e., how accurately it could locate a leak in the liner. Outside dimensions were established at 10 feet on each side, for a total lined floor area of 100 ft^2. Maximum depth was established at one foot, allowing variation of water depth during the experiments. A black polyethylene sheet 6 mils thick was selected as the geomembrane.

Instrumentation--

The instrumentation used to perform the test measurements is shown in Figure 6. A block diagram of the instrumentation is shown in Figure 7. The

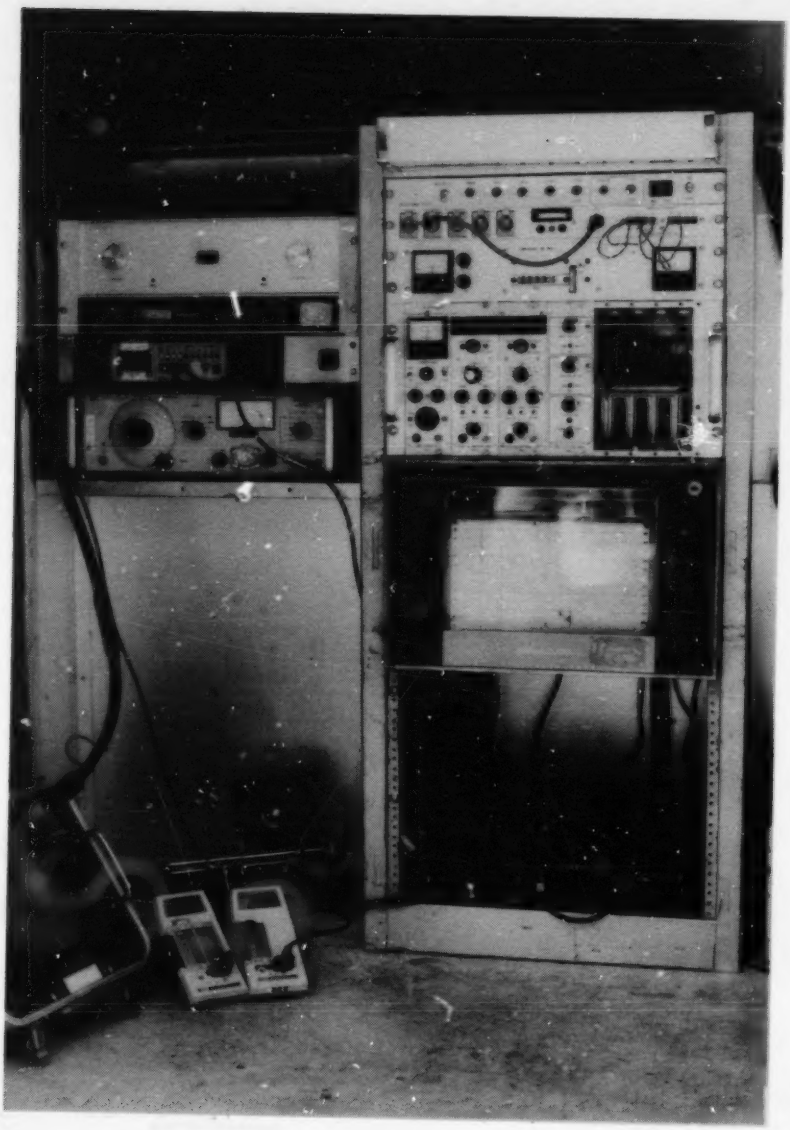

Figure 6. Instrumentation used to conduct physical scale model tests.

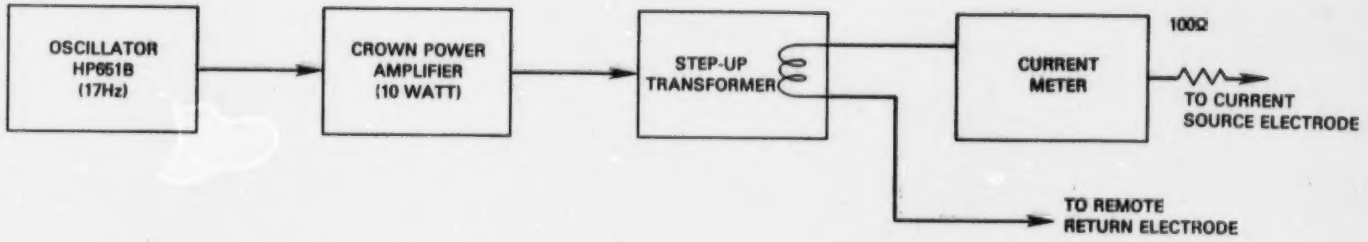

Figure 7. Block diagram of instrumentation used to conduct model tests.

equipment includes an oscillator to generate AC injection current at a frequency of 17 Hz or 25 Hz. A power amplifier increases the power of the oscillator output to 10 watts. The step-up transformer takes the output of the amplifier and drives the current into the liner model. A current meter wired in series with the source electrode is used to measure the injected current.

The model was constructed outdoors and contained a plastic liner. The model is shown in Figure 8. It was constructed in a square with 2 x 12 foot boards, each 10 feet long. A 6-mil polyethylene sheet was installed as the liner. To simulate the electrical shunting effect of a soil cover over the liner, 1000-ohm resistors along the edge of the model connected the water and soil inside the liner to the earth outside the liner. These resistors are shown in Figure 8 along the sides of the model.

Data Measurements--

Two electrodes were connected to the outputs of the AC current source. The source electrode was placed at the center of the fiberglass beam shown in Figure 8. This electrode was inserted into the water and soil fill during the studies to inject current. An infinity electrode was driven into the earth approximately 300 feet away from the model. This distance was sufficient to be considered at effective infinity with respect to the scale model.

Surface potential measurements were made using the fiberglass beam which supported 52 electrodes spaced 2.5 inches apart. The fiberglass beam and potential electrodes are shown in Figure 9. The stationary reference electrode was positioned in the corner of the scale model. Potential measurements were made between each of the electrodes on the fiberlgass beam and the reference electrode.

To obtain measurements, the fiberglass beam supporting the potential measuring electrodes was positioned across the water surface with the current injection electrode located on the beam. The beam was rotated around the pond at 10° increments, beginning with 0° and ending at 340°. For each placement of the beam, potential data were obtained by making measurements at increasing radial distances away from the current injection electrode. By rotating the beam 10° about the current injection point after measurements were obtained, measurements covering the entire surface of the scale model were obtained. Figure 9 shows a technician taking measurements along the fiberglass beam.

A total of 34 sets of surface potential measurements were obtained using the scale model, 23 with water fill and 11 with soil fill. The water-filled measurements were designed to simulate a fluid surface impoundment. The soil-filled measurements were designed to simulate a landfill.

Measurements were made with no leaks, one leak, and two leaks. Leaks were created by driving a 1/2-foot diameter copper clad steel stake through the liner into the soil underlying the liner. This stake provided a good conducting path between the water or soil and the earth, while minimizing the loss of water.

Figure 8. Physical scale model showing the plastic liner and shunt resistors.

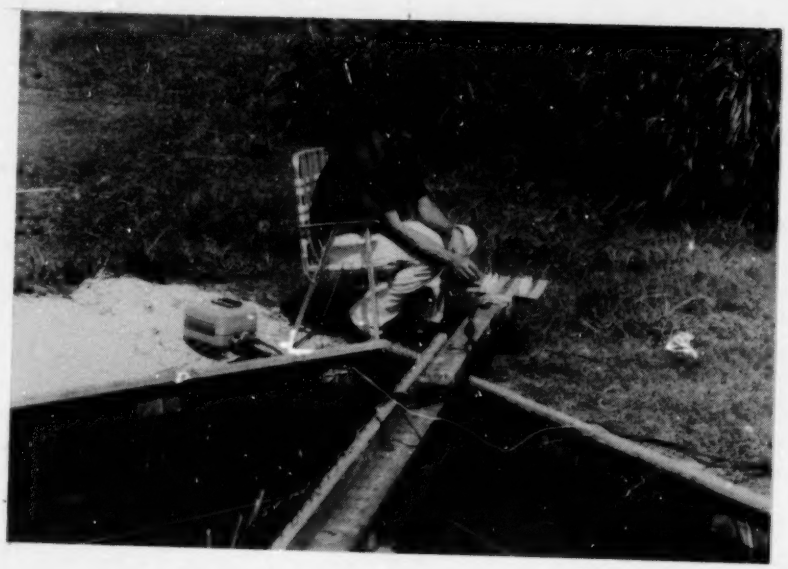

Figure 9. Potential measurements being taken using the fiberglass beam which supports electrodes.

The water level was varied from 3.25 to 8.75 inches. This was done to observe the influence of water depth on leak signatures. A metal block was placed in the water for five measurement sets to observe the influence of a highly conductive anomaly on leak detection and location.

After water-filled tests were completed, the model was drained and 2.75 inches of soil were placed into the model. Three tests were performed at this depth. Additional soil was added until the depth was 5.5 inches. Five tests were conducted at this depth. The remaining three tests were performed with a soil depth of 10 inches. A new current electrode constructed from one-half of a metal sphere approximately 3 inches in diameter was used for the soil tests. The increased surface area of this electrode over the rod shaped water electrode provided good current injection stability.

All 34 tests were run with the current shunts in place. This simulated the possible effects that a soil cover over a liner would have on the current flow. It was anticipated that leak detection and location would be more difficult with these shunts in place. Their effect would be to diminish the flow of current through a leak, thus reducing the strength of the leak signature.

Results--

Surface potential measurements were made with 4 inches of water in the scale model. Figure 10 presents a polar coordinate equipotential plot of the measured data from one experimental configuration. The current injection electrode is shown in the center of the plot. A leak is shown on the 340° radial. The distortion of the equipotential lines indicates increased flow of current around the leak.

Figure 11 is a similar plot for a different current electrode position. The current injection point is toward the corner of the coordinate plot. To examine the influence of a highly conducting metal object on the leak signature, an aluminum block was positioned along the same radial between the current injection point and the leak. The equipotential lines exhibit the same distortion characteristics as shown in Figure 10. No observable distortion was created by the aluminum block. This test was one of five experiments performed using the aluminum block. All five tests confirmed that the conducting block did not noticeably affect the experimental signatures of leaks in the liner.

Figure 12 shows the influence of a leak near the edge of the liner on the surface equipotential contour lines. This plot demonstrates the fact that the edges of the liner do not interfere with leak detection. This was an important determination as part of the process of defining the limitations of the technique.

Figure 13 shows a plot with two leaks on radials 20° apart. The equipotential lines were distored by both leaks. This test was conducted with 4 inches of water in the model. Figure 14 shows a similar two-leak test, with the leaks on radials 40° apart. Here both leaks exhibit similar distortions of the contour lines.

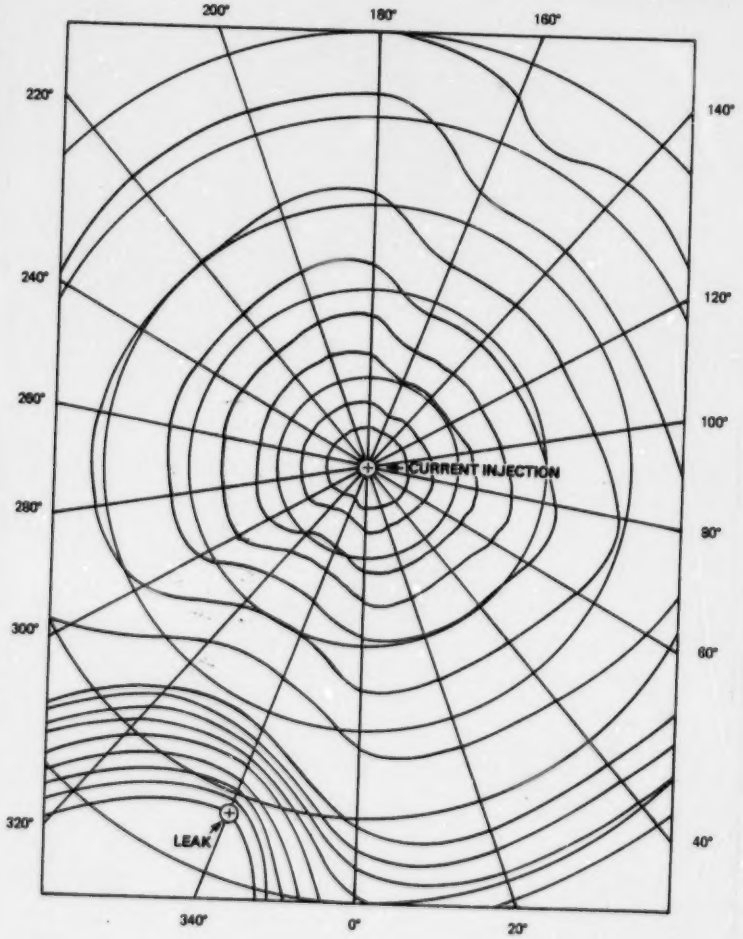

Figure 10. Equipotential plot of voltages on the surface of the water with a single leak.

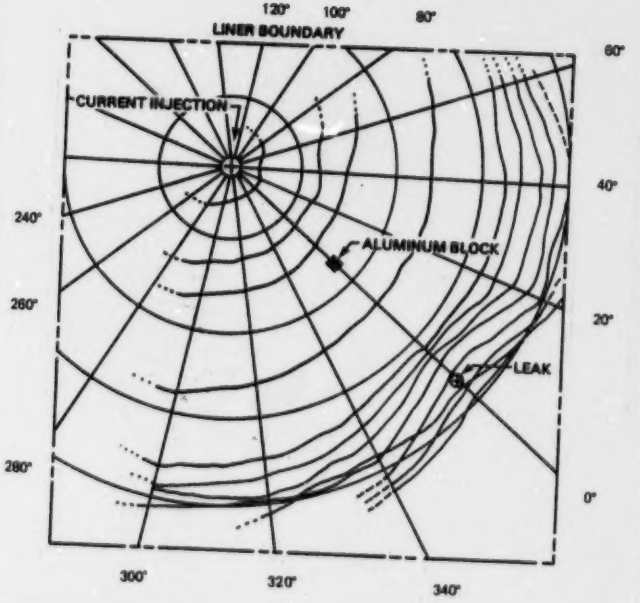

Figure 11. Equipotential plot of voltages on the surface of the water with a highly conductive aluminum block and one leak.

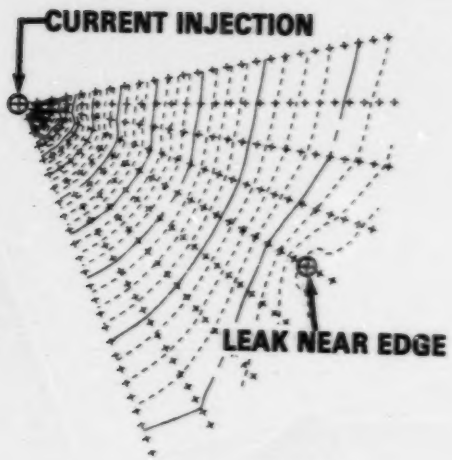

Figure 12. Equipotential plot of voltages on the surface of the water with a single leak near the edge of the liner.

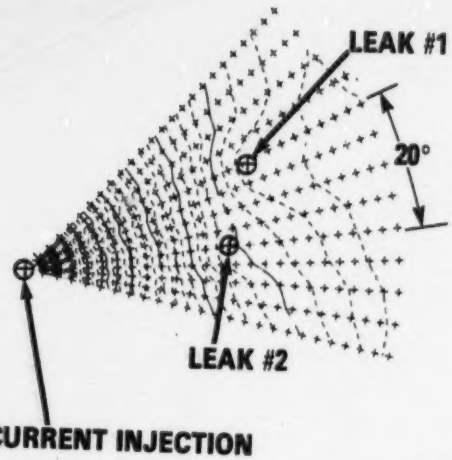

Figure 13. Equipotential plot of voltages on the surface of the water with two leaks 20° apart.

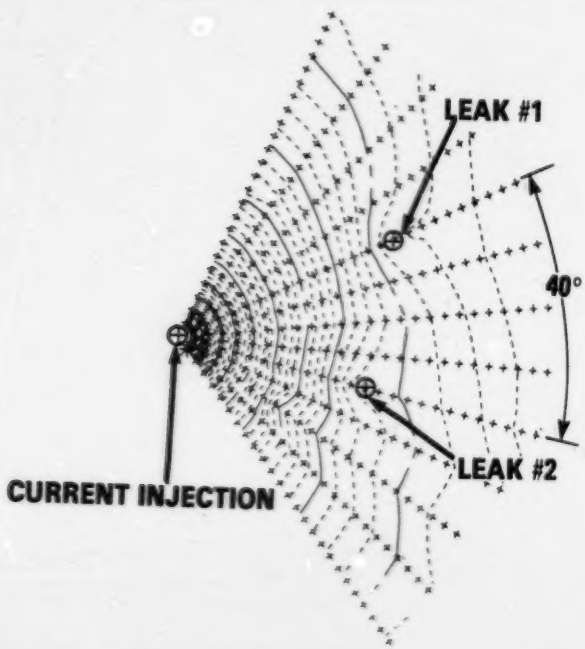

Figure 14. Equipotential plot of voltages on the surface of the water with two leaks 40° apart.

To assess the impact of increased water depth on the leak signatures, the water level in the model was increased to 9 inches. The results of this test at the increased water level are shown in Figure 15. As shown, the contour lines are less distorted with the deeper water. However, the distortions are evident for several contour lines closer to the current electrode than with the shallower water fill. This suggests that the signatures of the leaks may be smaller in magnitude but larger in areal extent as water depth is increased.

Testing on the water-filled model (simulating a fluid impoundment) confirmed that leaks can be detectd and located with the technique. To determine if the system would achieve the same performance on a simulated landfill, the water in the model was replaced with a sandy loam. Figure 16 presents the results of a test with 2.75 inches of soil in the model and one leak. The current injection electrode is shown in the center of the plot. The equipotential contours are distorted in the area of the leak as with the water-filled condition. The same test was performed after the soil depth was increased 100 percent to 5.5 inches. Figure 17 shows the results of this test. The contour lines close around the leak location, clearly identifying its location.

To determine the influence of two leaks with soil fill, a test was performed with two leaks on radials 40° apart. The depth of soil was 5.5 inches. Figure 18 shows the location of the leaks and their influence on the equipotential contour lines. Both leaks can be clearly identified on the plot by the distortions in the contour lines.

These studies further demonstrated the fundamental concepts of this approach which were first defined by the computer modeling efforts. Based upon these results, the measurement equipment, data processing software, and electrodes were specified for testing at a 1-acre lined facility located on Institute grounds. Testing at this scale was performed to measure the performance of the technique at conditions which more accurately simulate actual field conditions. The design of the 1-acre facility, instrumentation specifications, and experimental procedures are presented in the following section.

LARGE-SCALE TESTING

The electrical resistivity leak detection technique was tested at a 1-acre lined water-filled impoundment. The overall goal of the testing program was to determine how well the technique worked under conditions simulating a field environment. To accomplish this goal, the instrumentation required to apply the electrical resistivity technique was assembled. A 100-mil geomembrane liner made of high-density polyethylene was installed in a 1-acre impoundment. Controllable leaks were installed in the liner for detection and location studies. Experiments were then performed to evaluate the technique and the instrumentation.

Impoundment Design

A 1-acre impoundment was utilized to test the liner assessment technique. The facility was designed to accommodate up to 6.5 feet of water. Figure 19 shows a plan view of the facility. Overall dimensions are approximately 216 feet x 216 feet from the top of the berms. Side slopes are approximately

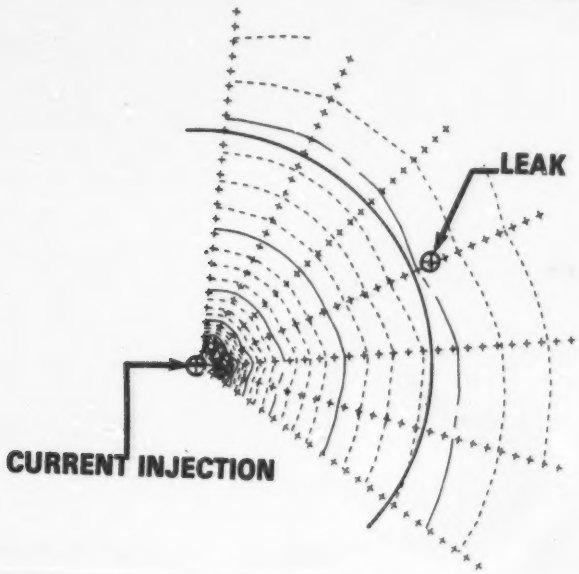

Figure 15. Equipotential plot of voltages on the surface of the water with a single leak.

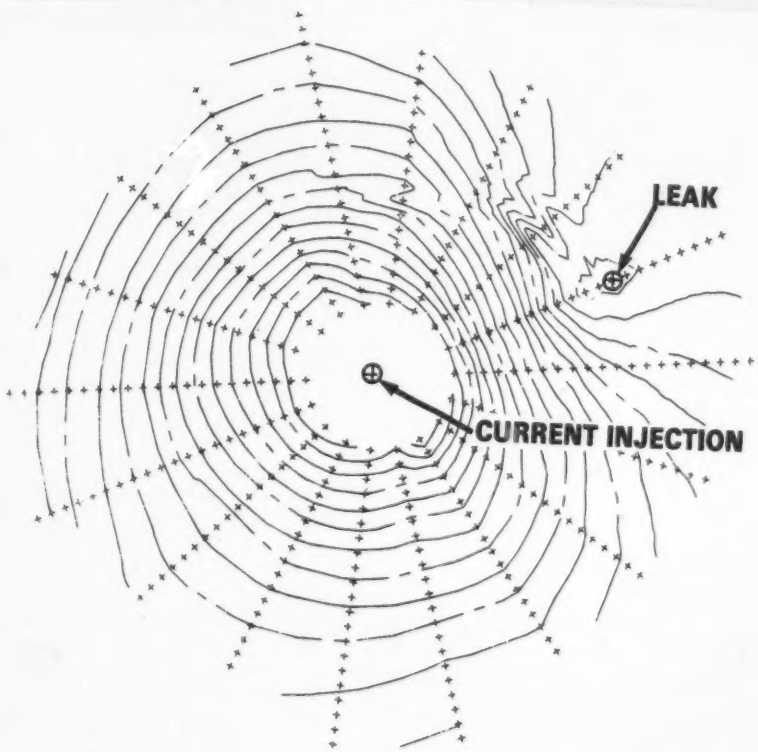

Figure 16. Equipotential plot of voltages on the surface of the soil with a single leak.

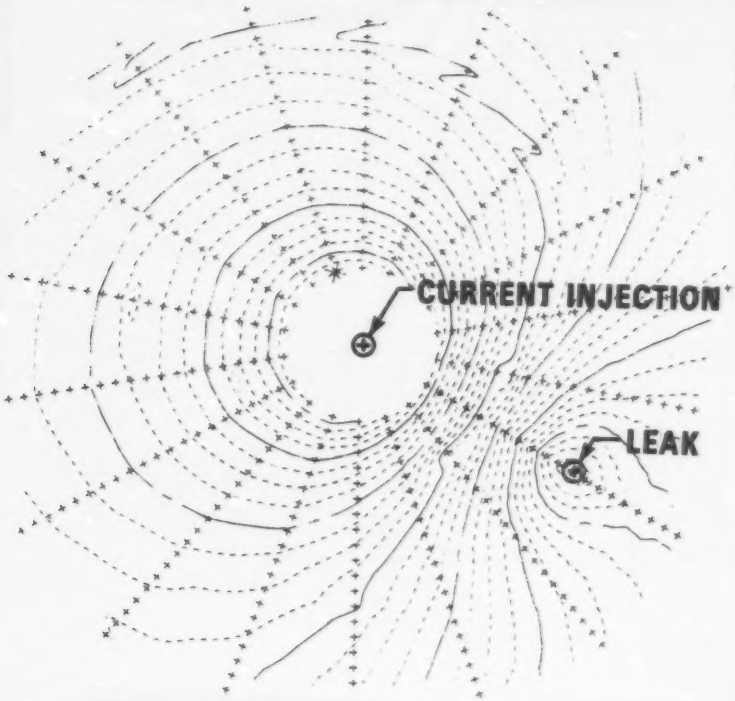

Figure 17. Equipotential plot of voltages on the surface of the soil with a single leak.

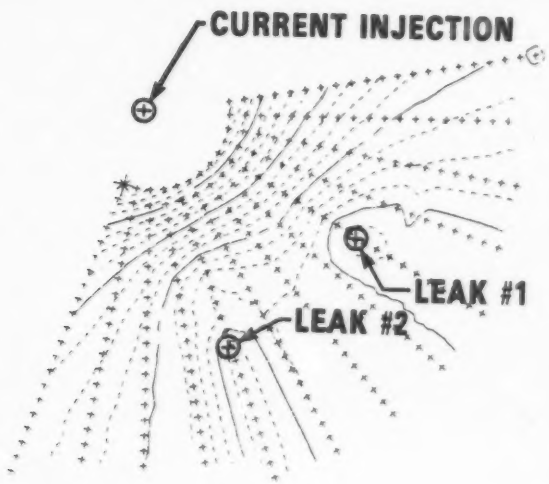

Figure 18. Equipotential plot of voltages on the surface of the soil with two leaks 40° apart.

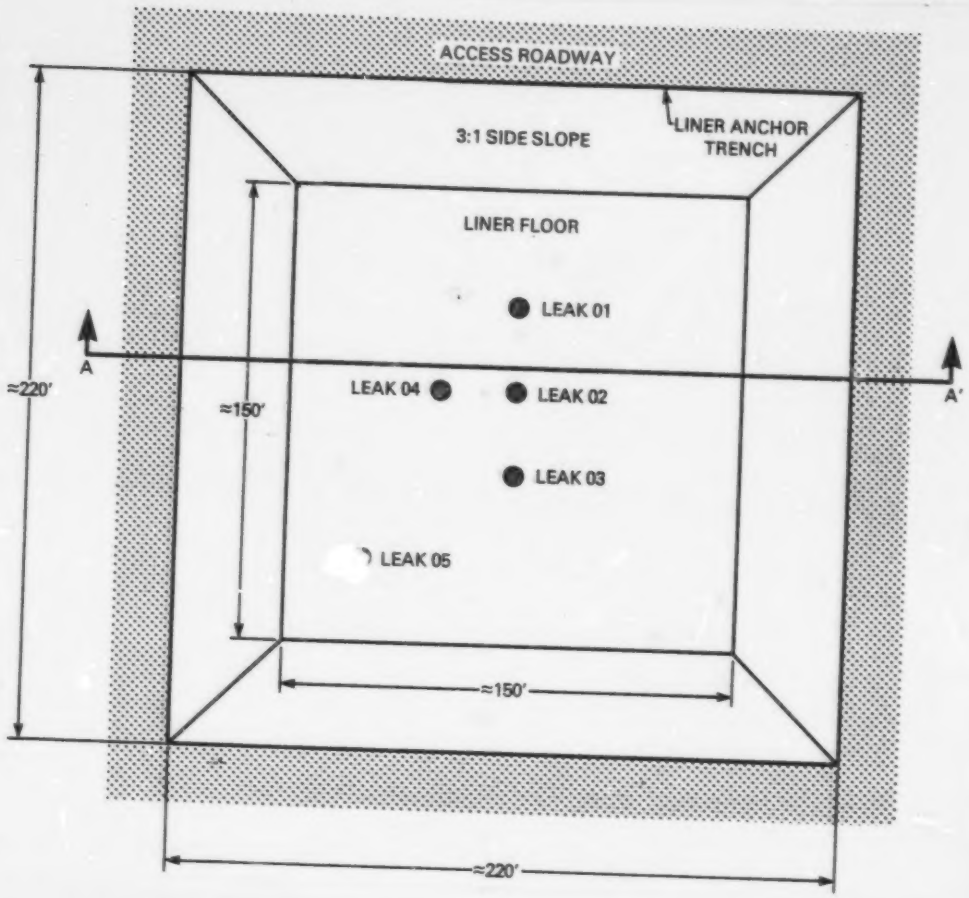

Figure 19. Plan view of the test impoundment.

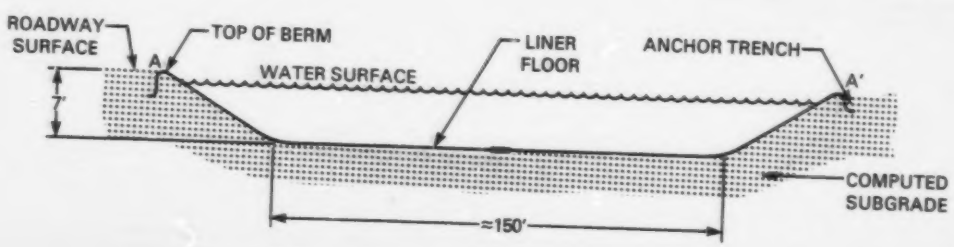

Figure 20. Cross section A-A' of the test impoundment.

three to one. A cross section is shown in Figure 20. An access road exists around the facility to allow for vehicular traffic during testing. Construction of the facility is shown in Figure 21.

A 100-mil high density polyethylene liner was installed in the facility to serve as the test liner. Installation of the liner is shown in Figure 22. The liner was anchored at the top of the berm in a two-foot deep trench. The trench was backfilled with soil.

It was necessary to construct leaks in the liner to facilitate testing of the leak detection technique. Five pipes, each one foot in diameter, were installed in the floor of the liner. Figure 23 shows the installation of one of these pipes. The pipe was made of HDPE to allow the liner to be welded to the pipe, creating a water-tight seal. A cap was constructed to fit over this pipe. The cap is made from two rings which are bolted together. To create various leak sizes, an HDPE insert was placed between the rings and then the rings were bolted together and placed over the top of the pipe. Figure 24 shows the rings and a plastic insert. Five of the pipes were installed in the liner at the locations shown in Figure 19. These leak points allowed control of leak location during the performance tests.

Instrumentation and Hardware

The instrumentation and hardware assembled to test the electrical resistivity technique at field conditions included various electronic instrumentation components, an electrically operated logging winch with 500 feet of cable, a support platform, and four electrodes of different designs.

Electronic Instrumentation--

Instrumentation requirements included a stable, low frequency, alternating current source; precision voltage sensing amplifiers; an analog-to-digital converter; and a data logging system capable of previewing the field measurements to an accuracy of 72 dB with a dynamic range of 120 dB. These requirements were based upon the results of the physical scale model testing and experience with other field resistivity measurement instrumentation. The measurement or receiver side of the instrumentation was designed to obtain data from the surface of the water, since initial tests were planned for a water-filled lined facility.

A simplified block diagram of the electronic components used during the tests is shown in Figure 25. The transmitter, consisting of a current source connected to two electrodes, provides the necessary current needed to generate potentials on the surface of the impoundment. The receiver measures the surface voltage potentials which are then analyzed to detect and locate leaks in the liner. The current source electrode is located in the water. The remote current return electrode is placed in the earth away from the impoundment.

Major components of the receiver include the System Control Unit and the Multiprogrammer. These two components provide for automatic data acquisition.

Figure 21. Test impoundment construction activity.

Figure 22. Liner installation activities.

Figure 23. Installation of an HDPE pipe designed as one of five leaks through the liner.

Figure 24. Rings used to hold plastic inserts designed as leaks.

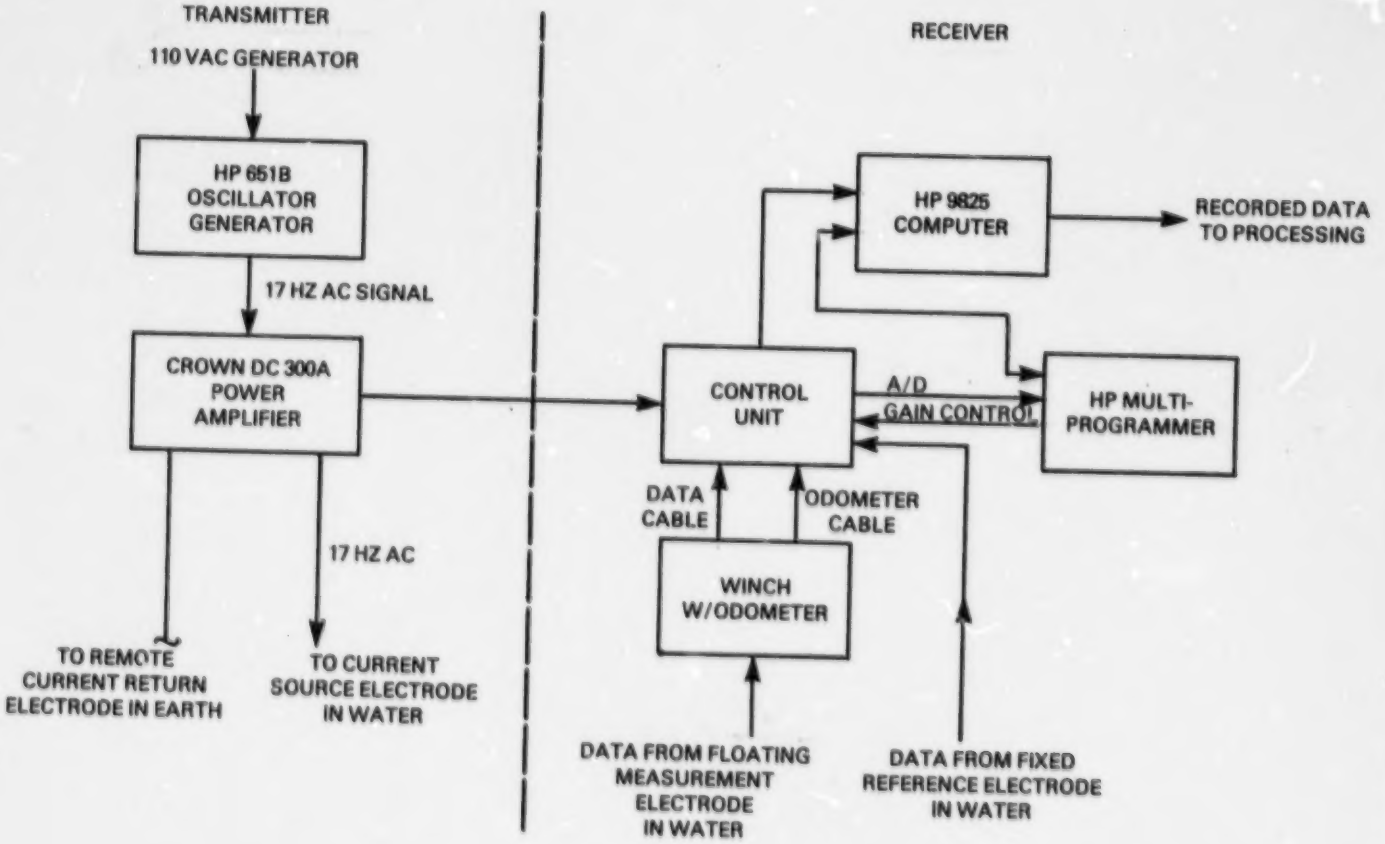

Figure 25. Simplified block diagram of the equipment used to test the electrical resistivity technique.

With the HP 9825 computer, the data is automatically stored on tape for off-site processing on an HP 9826 computer and associated printer-plotter.

As indicated in Figure 25, measured surface potential voltages are sent in analog form via cable through the winch to the system control unit. The control unit sets the signal gain, filters the signal to remove ambient noise, and generates a DC voltage proportional to the magnitude of the AC signal measured by the potential electrode. The DC signal is coupled to a 12-bit analog-to-digital high speed converter in the Multiprogrammer. The digital output is then sent to the HP 9825 computer for display and storage on magnetic tape. The recorded data is processed off-site using an HP 9826 computer.

The instrumentation is operated from a mobile field laboratory. The laboratory is equipped with an onboard generator powered by a gasoline engine. This generator supplies 60 Hz AC power required to operate the instrumentation. The mobile laboratory is shown in Figure 26. The instrumentation inside the trailer is shown in Figure 27. The HP oscillator and crown amplifier are on the left. The system control unit and HP Multiprogrammer are shown to the right. The oscilloscope is used to monitor output voltages. The HP 9825 computer, to the far right, records field data on magnetic tape for off-site processing.

Electric Logging Winch--

An electric logging winch is used to control the location of the potential measuring electrode on the surface of the water. The winch is equipped with variable speed control, a photoelectric odometer, and an electric slip-ring. The winch drum, powered by the mobile laboratory AC generator, is equipped with 500 feet of data logging cable. The cable is reeled in and out to make surface potential measurements. The potential electrode is attached to the end of this cable. The odometer reading is monitored by the computer and its value, which indicates the position of the measurement electrode, is used to determine when to trigger a new potential reading. The odometer allows calculation of the location of leaks and therefore is a critical measurement system component. The winch is shown in Figure 28.

System Electrodes--

The liner testing system requires the use of a current source electrode, a potential reference electrode, a remote current return electrode, and a floating potential measurement electrode. The current injection electrode is a 3-foot diameter brass disc 1/16 inch thick. It is mounted on a platform which extends out into the pond. The electrode is positioned 3 to 4 inches below the water surface, directly above the bottom of the pond side slope. Brass was selected for the electrode due to its excellent conductive properties and resistance to corrosion. The large diameter of the disk increases the surface area and reduces the voltage drop between the electrode and the water. The circular shape is compatible with the polar coordinate data acquisition system and helps reduce voltage anomalies in the region of the electrode. Electrical current is applied to the electrode via a wire from the output of the current source in the trailer. A photo of the current source electrode is shown in Figure 29.

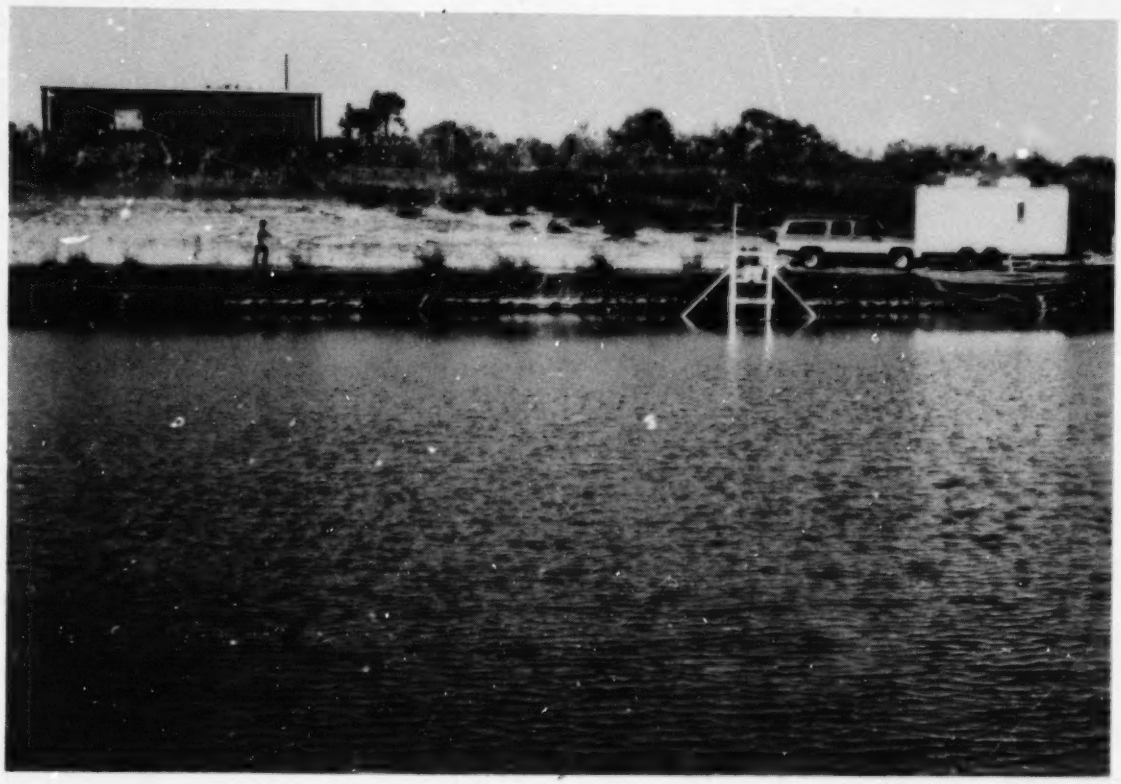

Figure 26. A mobile laboratory trailer, shown at the upper right, is used to house the instrumentation during testing.

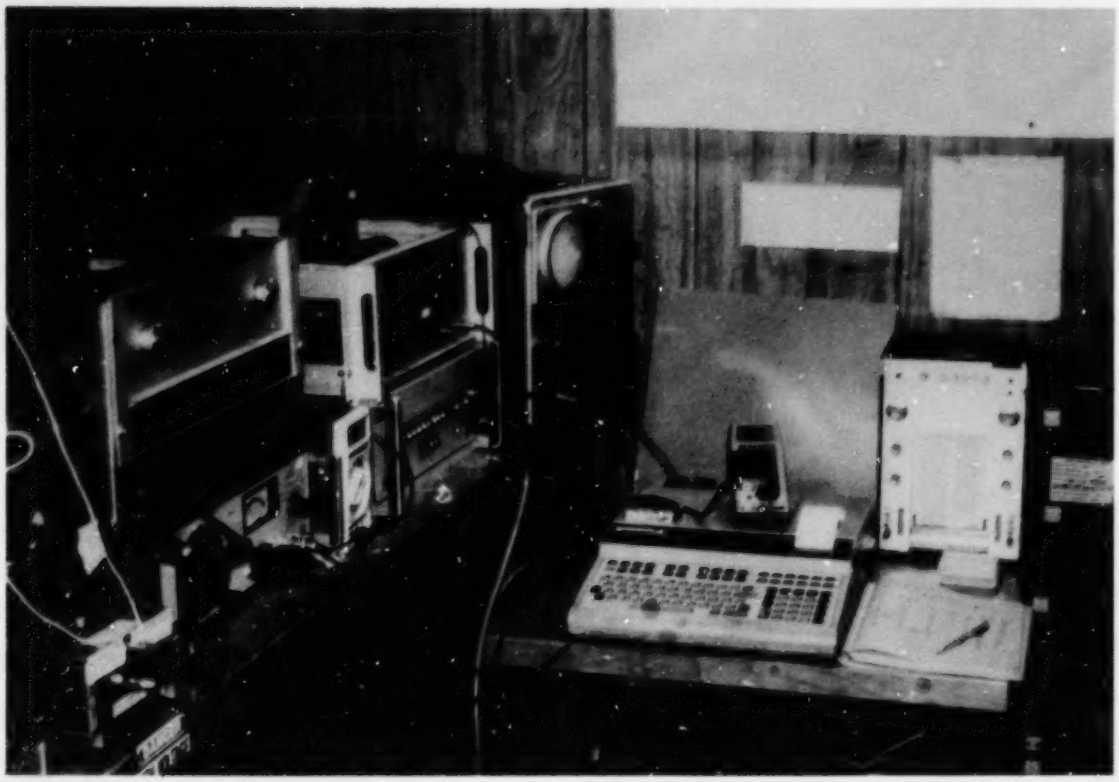

Figure 27. Testing instrumentation inside the mobile laboratory.

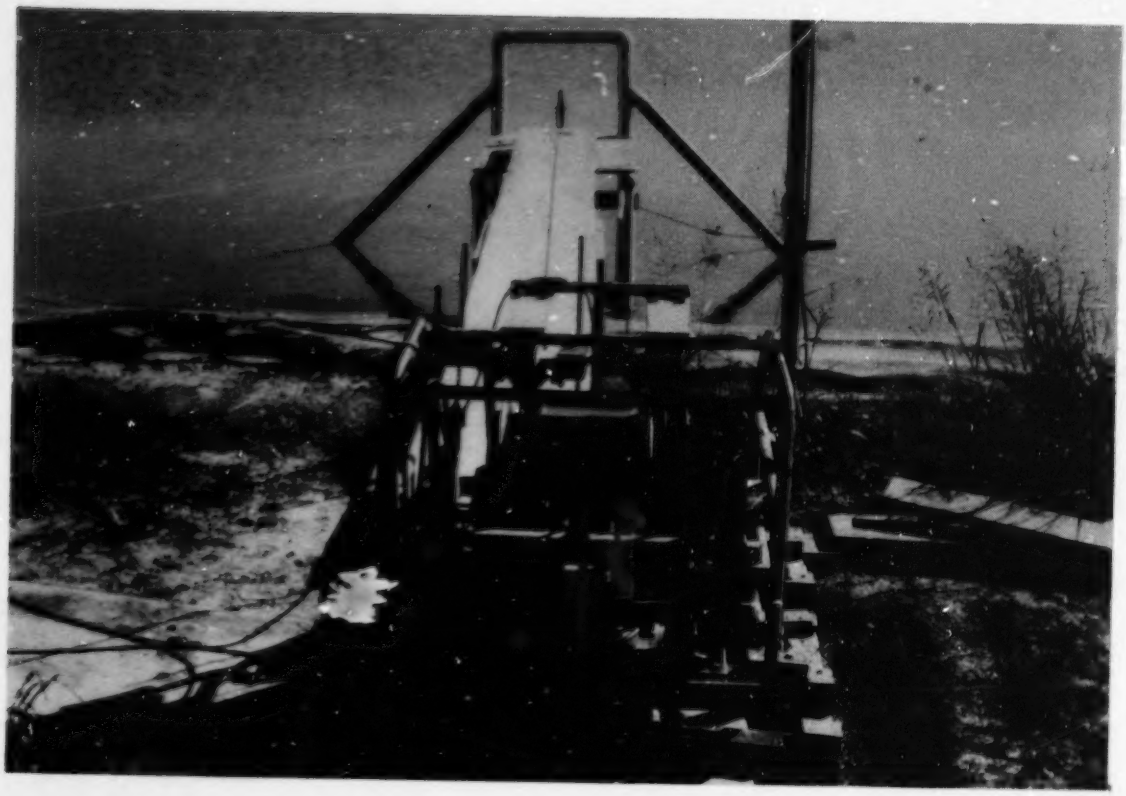

Figure 28. The electrically operated logging winch used during testing to control the location of the measurement electrode.

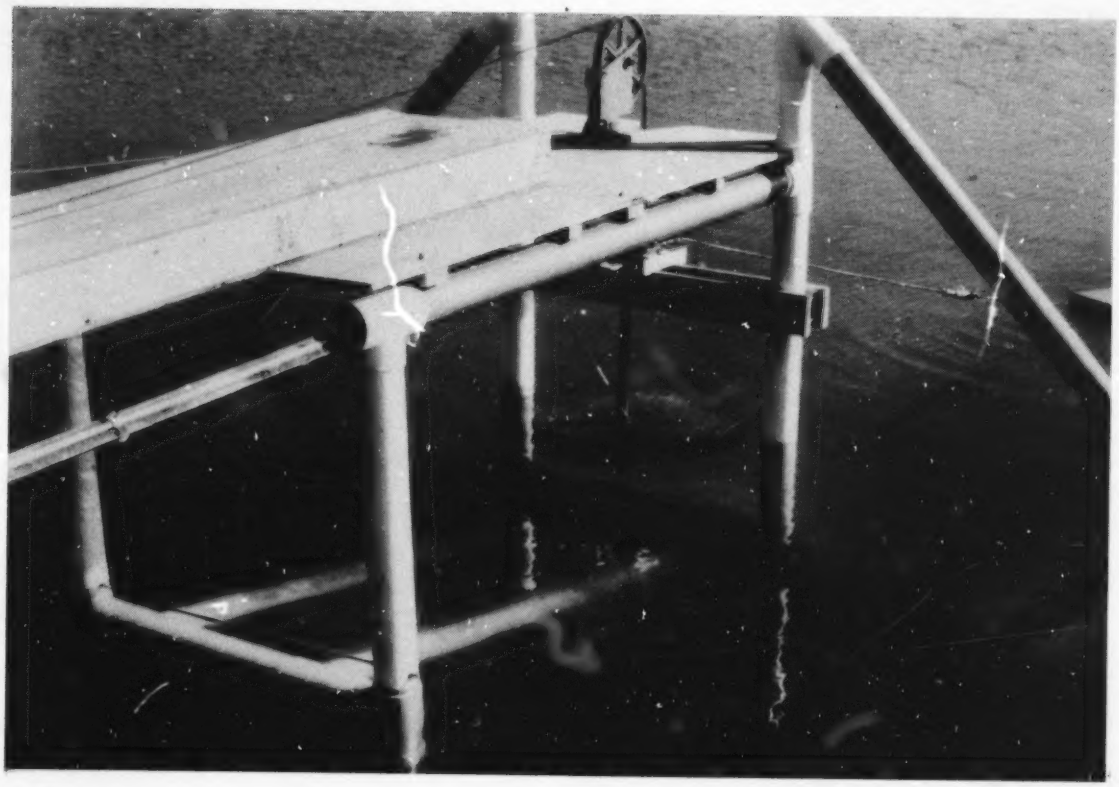

Figure 29. The circular brass disc below the end of the platform is used at the current source electrode during testing.

The remote current return electrode consists of three copper clad steel stakes driven into the earth to a depth of 36 inches and wired together using a common conductor. The three stakes, which are approximately one foot apart, were used to increase surface area and reduce the voltage drop between the electrodes and the earth. The electrodes are located 600 feet to the north of the test impoundment.

Surface potential measurements are made using a stationary reference electrode and a mobile potential electrode which is floated on the surface of the water. The reference electrode is a copper bar approximately 1.5 feet long, 2 in. wide and 0.25 in. thick. This electrode is positioned below the water surface on the side slope of the pond adjacent to the platform. During operation of the testing system, this electrode remains stationary, serving as a reference point. All surface potential voltage measurements are made with respect to this electrode. A preamplifier with unity gain is wired in-line between this electrode and the system control unit. The preamplifier serves as an impedance matching circuit and electrical buffer to the control unit. The reference electrode and preamplifier are shown to the left in Figure 30.

The potential measurement electrode consists of a plastic box approximately one-foot square with a preamplifier mounted inside. A 5-inch welding rod 1/16 inch in diameter is inserted into the bottom of the box, directly into a connector in the preamplifier. Figure 30 shows this potential measurement electrode box. The electrode is visible, protruding up from the center of the box. The preamplifier contained in the box is identical in design and function to the one used for the reference electrode.

Potential Measurement Procedures--

The operation of instrumentation and hardware is shown in the conceptual drawing in Figure 31. The step-by-step procedure for measuring surface potentials on the water is as follows:

(1) Position all electrodes and check cables and connections for proper installation.

(2) Clean electrodes in the water to eliminate possible deposit buildup.

(3) Bring instrumentation up to stable operating conditions.

(4) Set the current source to the appropriate current output (normally 0.05 ampere).

(5) Position the potential measurement electrode at a selected reference odometer reading (usually 6.0 feet from the current electrode).

(6) Load operating program and data tape into the HP 9825 computer.

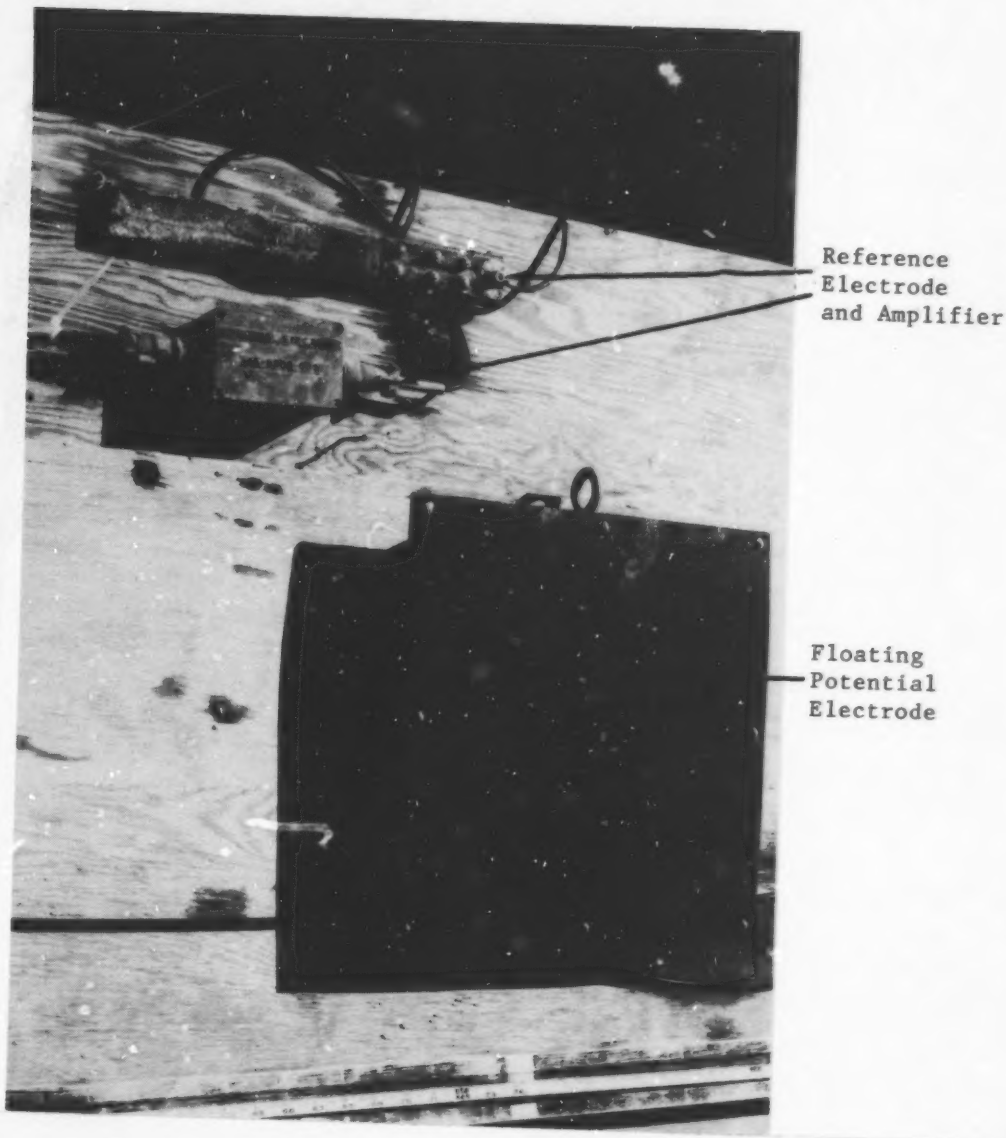

Figure 30. The reference electrode and preamplifier housing are shown to the left of the potential measurement electrode box.

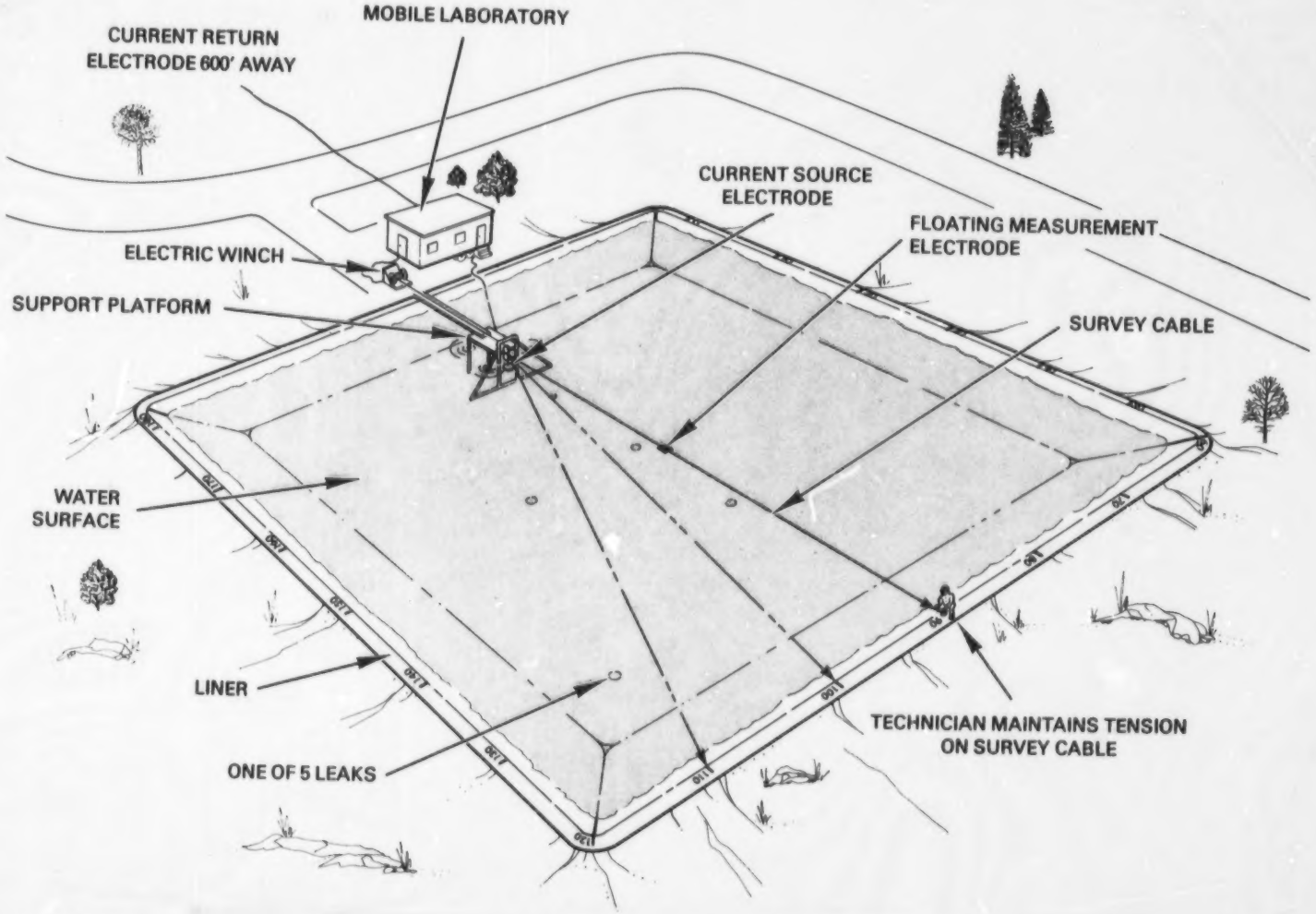

Figure 31. Conceptual drawing of the test impoundment and operation of the test equipment.

(7) Manually pull the floating potential electrode away from the current electrode, along a preselected measurement line, to the desired location where measurements are to begin.

(8) Set the computer to receive and record data.

(9) Turn on the winch motor and reel the potential electrode back to the initial starting point.

(10) Manually maintain tension on the cable during winch operation to prevent cable fouling.

(11) When the potential electrode returns to its original position, reset the computer.

(12) Manually move the rope attached to the potential electrode along the berm of the pond to the next measurement line.

(13) Repeat steps (5) through (11) for each survey line.

The HP 9825 computer controls the recording of measured data. During step (6) listed above, the computer will prompt the operator for the following input data: current injection position, water depth, leak location, logging interval, current water temperature, wind velocity, and relevant remarks. After appropriate responses are entered, the computer will then instruct the potential electrode to be positioned. After this is performed, the computer will record data. The winch is switched on and the electrode is pulled out and into position. The computer is reset to log data, and the winch is started to reel the electrode back toward the current electrode. The entire procedure is repeated for each survey line.

SECTION 5

RESULTS AND DISCUSSION

OVERVIEW

All measurements at the one-acre test impoundment were taken along radial lines 5° or 10° apart, beginning at the current source electrode out to markings on the berm. The 0° through 180° radial lines were located by marking the liner as was shown in Figure 31. To mark the berm, a transit was positioned over the current source electrode. The angle marks were painted on the liner at 5° increments, starting at 0° to the left around 180° to the right. The logging cable was positioned on these marks during data acquisition runs. The location of any anomaly, such as a leak, could be calculated from the radial and the odometer data. To establish a baseline condition, the entire surface of the pond was surveyed with all leaks closed. Then, various leaks were created through the liner and measurements taken. A contour plotting computer program was used to produce equipotential contour plots of the no-leak and leak data. The results of the testing are presented in the following sections.

NO-LEAK SURVEY RESULTS

The computer generated plot shown in Figure 32 presents the no-leak baseline surface voltage potentials measured along the radial. The solid curve shows the measured no-leak condition surface potential voltages at the corresponding odometer readings. The dotted curve is a least square curve fit to the measured data. The minimum voltage shown on the plot near an odometer reading of 17 feet occurred when the measurement electrode passed over the reference electrode. Subsequent to this measurement run, the reference electrode was moved closer to the current electrode to prevent this null from occurring. No other perturbations along this radial were observed, indicating that no anomolies such as a leak were detected. These data are typical of the no-leak data obtained for other radial lines across the surface of the water.

A contour plotting computer program was used to produce an equipotential contour plot of these data. The data presented in Figure 32, along with similar data for the other radial lines, were processed by the contour plotting program to produce the equipotential lines shown in Figure 33. The X and Y axes define the approximate north and east water level boundaries of the impoundment. The angles of the radials are indicated. The current source electrode is identified by a dot above the X axis at the 92-foot point.

The equipotential contour lines show insignificant distortions of the surface potentials across the water surface. These results are similar to the

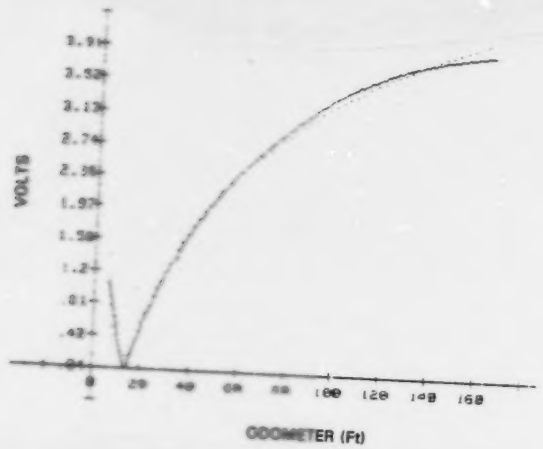

Figure 32. A plot of the potential measurements taken along the 90° radial for a no-leak case.

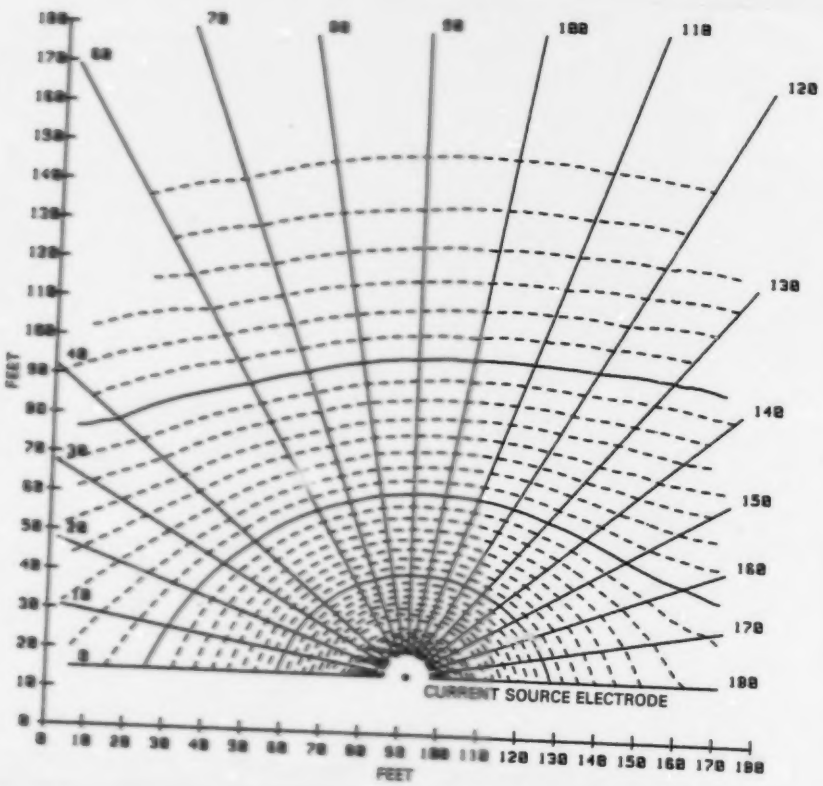

Figure 33. An equipotential contour plot of no-leak measurements.

no-leak contour plots of data taken with the physical scale model. The contour lines tend to be concentric semicircles close to the current injection point. Moving away from this region, the contour lines begin to straighten out, due to the effect of small amounts of current flow across the liner. Part of this current flow is due to the capacitive effects of the liner. Overall, this plot indicates no sudden, unexpected changes or perturbations in the current flow on the surface of the water.

ONE-LEAK SURVEY RESULTS

To determine if the survey technique could detect and locate a single leak, a one-foot diameter (0.79 ft^2) leak in 5 feet of water was opened. The surface potentials were measured and the results plotted as before. The solid line in Figure 34 is a plot of the measured data along the 90° radial. Examination of this plot indicates a peak in the surface potentials occurring at an odometer reading of approximately 72 feet. Based upon the conceptual and physical scale model studies previously conducted, this peak should occur near a leak location. The actual leak location in the pond was along the 90° radial, 72.3 feet from the current source electrode. Thus, the results of this experiment demonstrate the success of this technique to detect and locate a one-foot diameter leak in 5 feet of water.

An examination of the equipotential contour plot in Figure 35 shows that the contour lines close around the location of the leak. This indicates that the flow of current converges in the area of the leak, shown by the "bull's-eye" pattern centered on the leak. The bull's-eye potential pattern located on the surface of the water serves to graphically reveal the location of the leak. The plots of the data for each radial along with the equipotential contour plots serve as excellent analytical tools to detect and locate a leak.

To determine if the technique could detect and locate a smaller leak size, a one-inch diameter leak (0.005 ft^2) was installed on the 90° radial 72.3 feet from the current electrode. Surface potential measurements were taken at one-foot increments along the 60° through 120° radials. Figure 36 shows the results of the measurement taken along the 90° radial. A small peak was observed on the 90° radial directly over the leak. The equipotential contour plot of these data shown in Figure 37 indicates a significant distortion on the 90° radial in the proximity of the true leak location. From these results, it appears that, as the defects are diminished due to increased water depth, a radial plot such as that shown in Figure 36 can be used to locate the leak with more accuracy than the contour plot. These results indicate that the electrical resistivity technique can be used to successfully detect and locate a 0.005 ft^2 leak in approximately 40,000 ft^2 of liner surface area to an accuracy of one foot. The contour line shifts along the 110° radial in Figure 37 do not indicate an anomaly, since the shift is consistently the same magnitude.

An experiment was performed to determine the response of the technique when a leak was located near the edge of the berm. Figure 38 is a plot of the data measured along the 115° radial. A one-foot diameter (0.79 ft^2) leak was located approximately 154 feet from the current source electrode. A peak potential reading occurred at an odometer reading of approximately 156 feet.

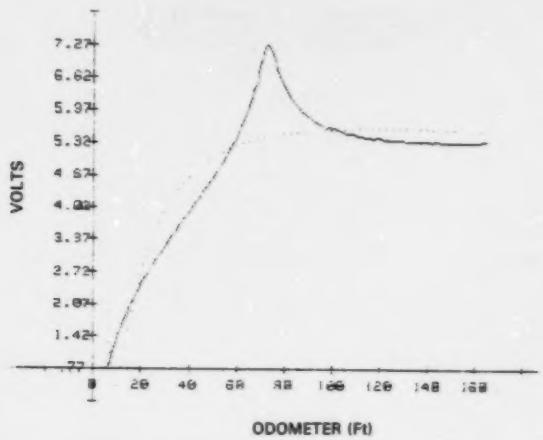

Figure 34. A plot of the potential measurements taken along the 90° radial. The peak occurs over a 1-foot diameter leak in approximately 5 feet of water.

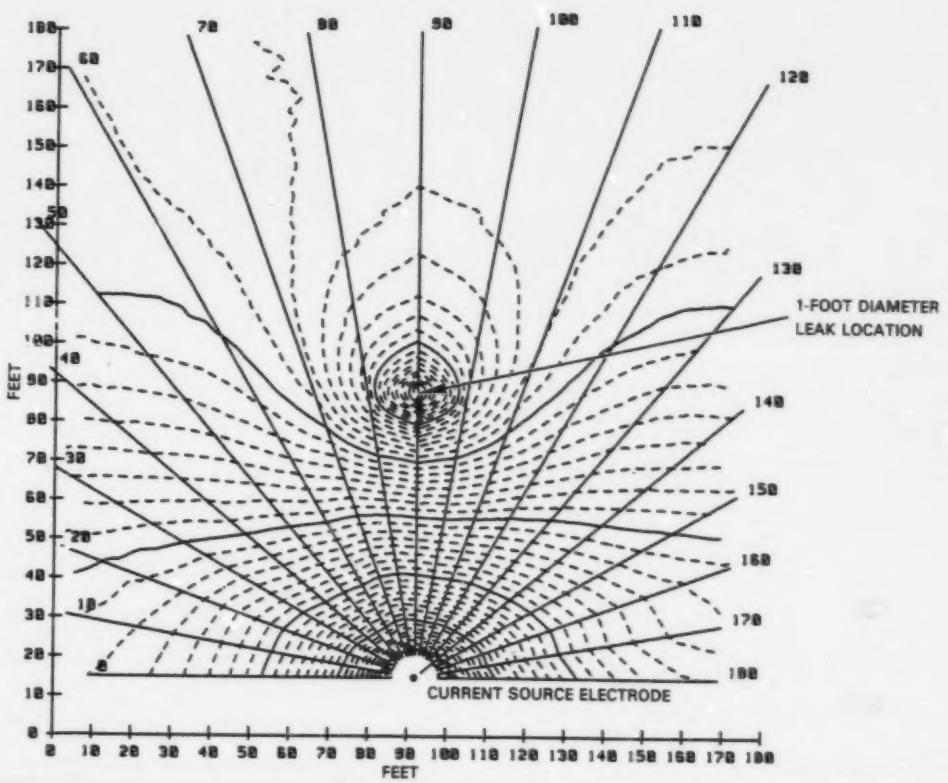

Figure 35. An equipotential contour plot showing the distortions from a 1-foot diameter leak on the 90° radial in approximately 5 feet of water.

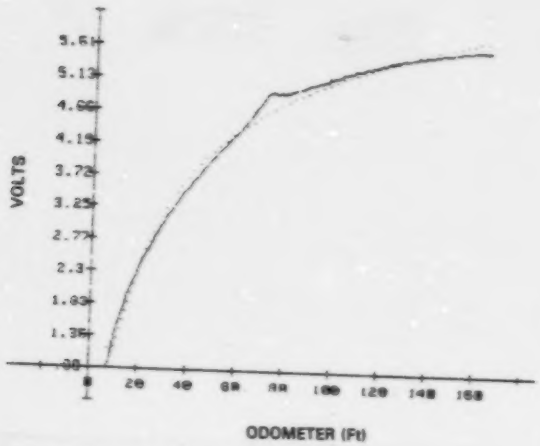

Figure 36. A plot of the potential measurements taken along the 90° radial. The peak occurs over a 1-inch diameter leak in approximately 5 feet of water.

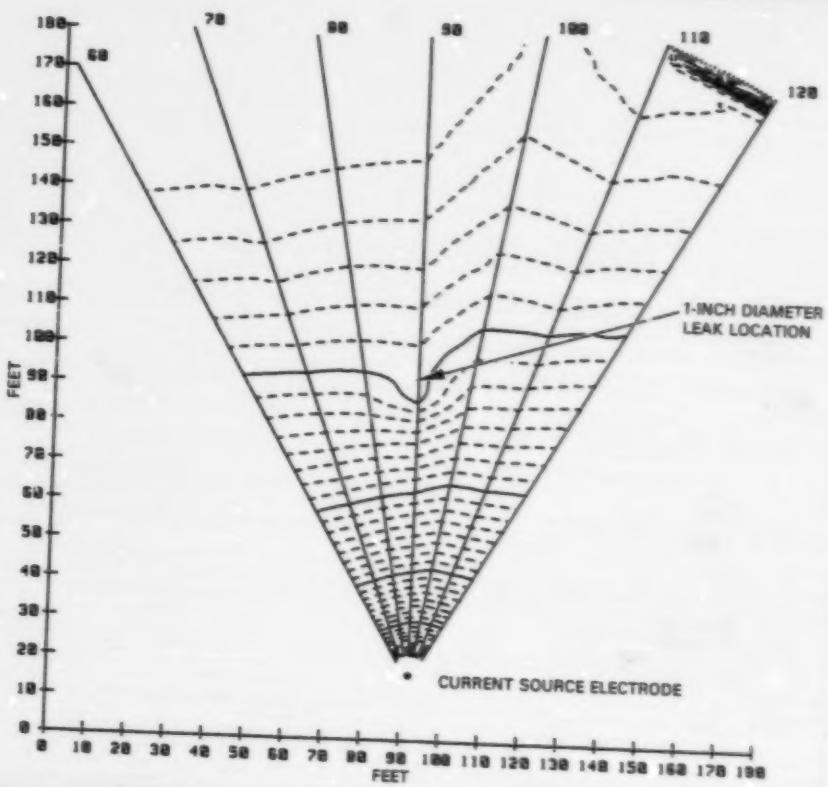

Figure 37. An equipotential contour plot showing the distortions from a 1-inch diameter leak in approximately 5 feet of water.

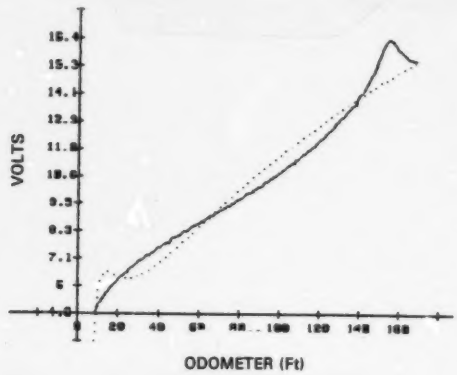

Figure 38. A plot of the potential measurements taken along the 115° radial. The peak occurs over a 1-foot diameter leak in approximately 5 feet of water.

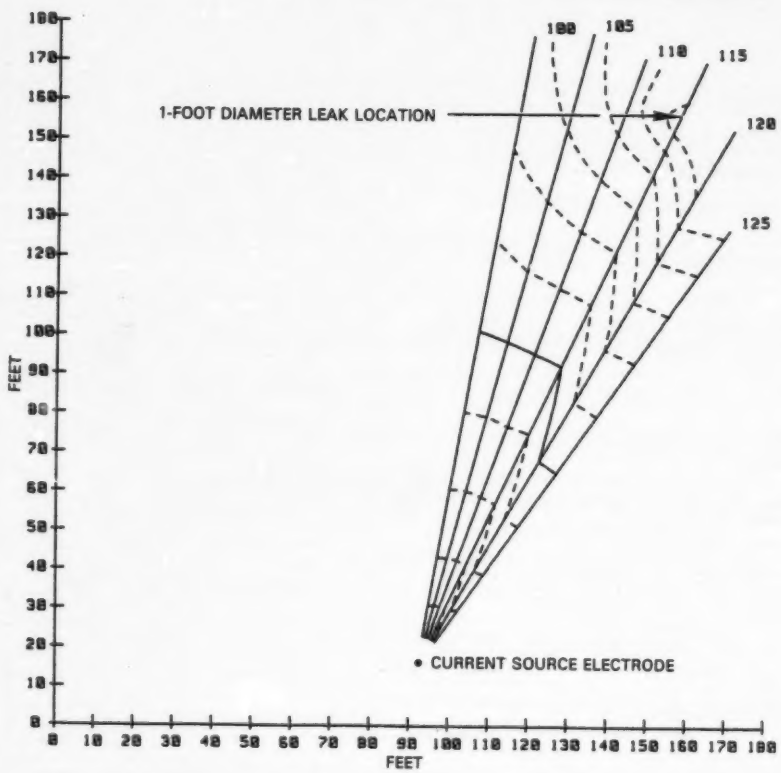

Figure 39. An equipotential contour plot showing the distortions from a 1-foot diameter leak in approximately 5 feet of water.

The equipotential contour plot of the data is shown in Figure 39. Distortions of the contour lines occur in the area of the actual leak location. There is an unexplained shift in the contour lines between the 115° and 120° radials. This may have been caused by a change in the current source output. However, the data suggest that leaks can be detected at this distance from the current source electrode and in close proximity to the edge of the liner. It was predicted that the berm of the impoundment would have an effect on the measurement results due to the resistive nature of the liner to current flow. This experiment indicates that the magnitude of this effect is small enough not to prevent detection of a leak this size. Subsequent tests with multiple leaks located near the berm substantiate this conclusion. These tests are described later.

SIMULATED LEAK SURVEY RESULTS

Tests were performed to determine if simulated leaks would produce results similar to actual leaks. It was desirable to use simulated leaks to add flexibility to the experimental testing of the technique.

The leak signature of a one-foot diameter (0.79 ft^2) leak located on the 90° radial 72.3 feet from the current source electrode in 5 feet of water is shown in Figure 40. The surface potential measurements peak at an odometer reading of 73 feet. The equipotential contour plot of these measurements, presented in Figure 41, clearly shows the presence and location of the leak.

A simulated leak of the identical surface area (0.79 ft^2) was fabricated from a brass disc. The disc was placed at the same location and grounded to the earth outside the liner. A plot of the measured potentials along the 90° radial is shown in Figure 42. This plot is identical in shape to the actual leak plot previously shown in Figure 40. The equipotential contour plot in Figure 43 clearly shows the location of the simulated leak. Based upon these results, it was concluded that simulated leaks could be used in place of actual leaks for testing of the electrical resistivity technique. The use of simulated leaks provided greater flexibility during subsequent testing of the technique.

Tests were run using simulated leaks to determine the influence of depth on the leak signatures. An examination of the potential data for the 90° radial shown in Figure 44 indicates a peak voltage of approximately 11.0 volts. Figure 45 shows the equipotential contour lines for a one ft^2 leak in 5 feet of water. The contour line intervals indicate a relatively high flow of current at the surface near the leak. Figure 46 presents the raw data for the 90° radial line for the same leak configuration. However, the water depth is 6.5 feet. Note that the voltage at the peak is 3.9 volts. The equipotential contour plot is shown in Figure 47. The contour line intervals indicate a lower current flow near the leak. These two tests were conducted at the same current source amperage and position of the current source electrode. These results suggest increased water depth reduces the surface potential voltages near a leak. However, in both cases, the leaks are clearly distinguishable from both the raw data plots and the contour plots. Leak signatures are not available for depths greater than 6.5 feet. Therefore, the exact influence of depth on signatures is unknown. It is indicated, however, that

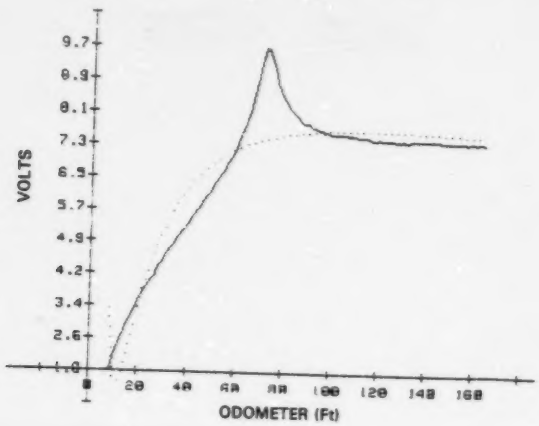

Figure 40. A plot of the potential measurements taken along the 90° radial. The peak occurs over a 1-foot diameter leak in approximately 5 feet of water.

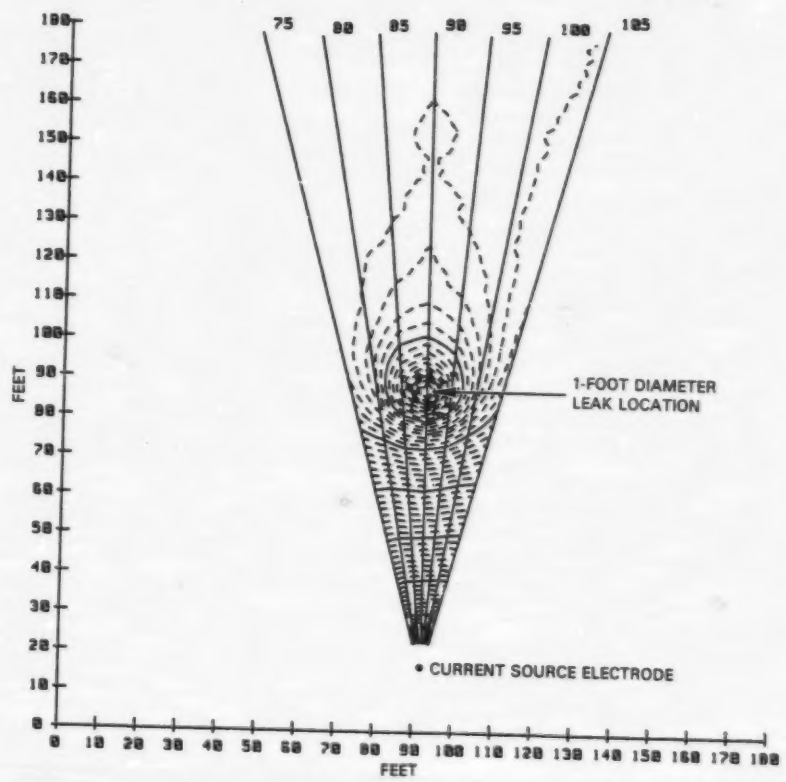

Figure 41. An equipotential contour plot showing the distortions from a 1-foot diameter leak in approximately 5 feet of water.

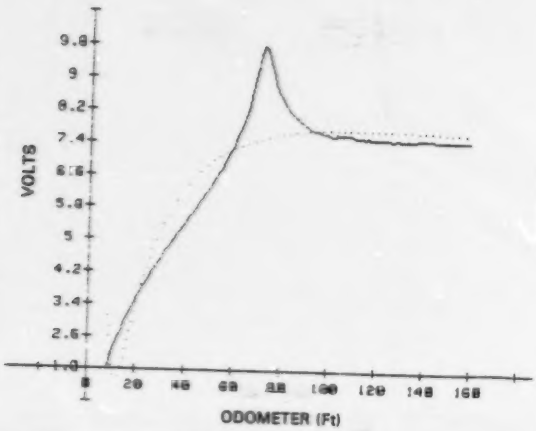

Figure 42. A plot of the potential measurements taken along the 90° radial. The peak occurs over a simulated 1-foot diameter leak in approximately 5 feet of water.

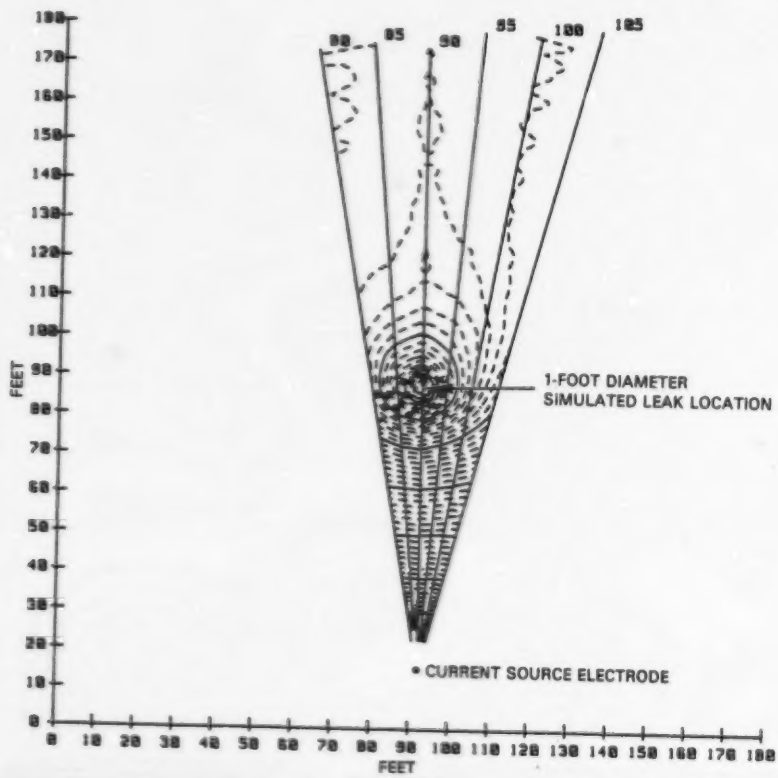

Figure 43. An equipotential contour plot showing the distortions from a 1-foot diameter simulated leak in approximately 5 feet of water.

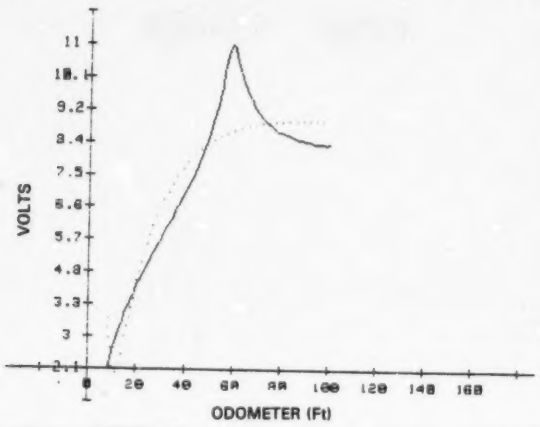

Figure 44. A plot of the potential measurements taken along the 90° radial. The peak occurs over a 1-foot square simulated leak in approximately 5 feet of water.

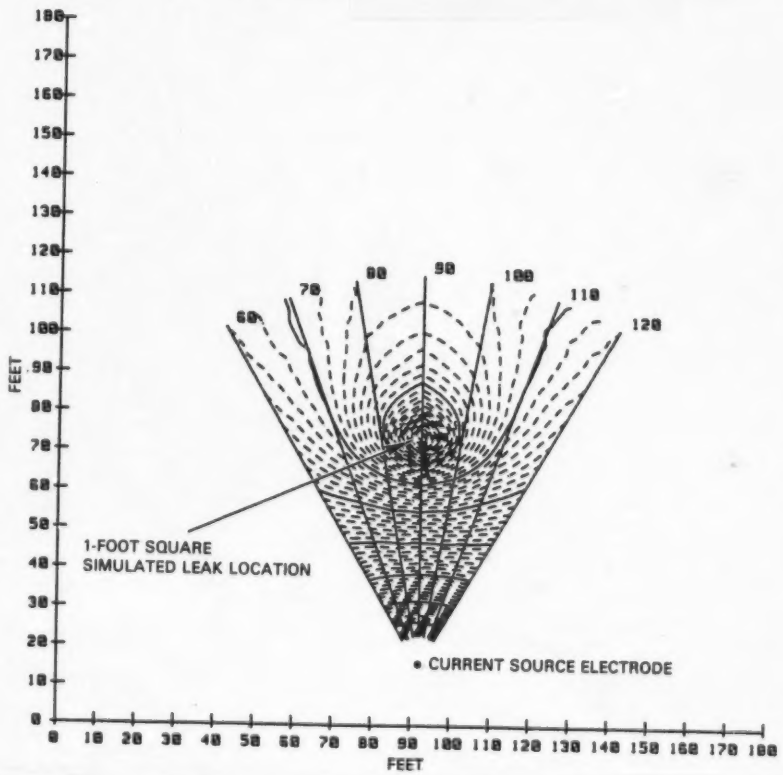

Figure 45. An equipotential contour plot showing the distortions from a 1-foot square simulated leak in approximately 5 feet of water.

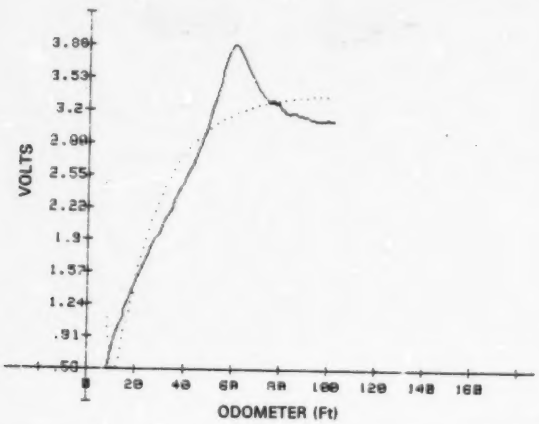

Figure 46. A plot of the potential measurements taken along the 90° radial. The peak occurs over a 1-foot square simulated leak in 6.5 feet of water.

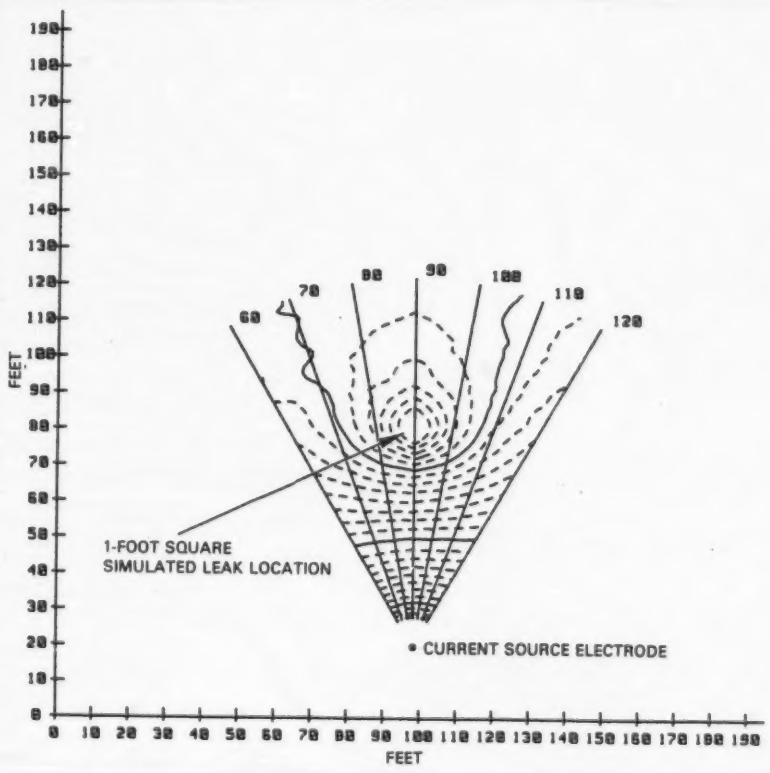

Figure 47. An equipotential contour plot showing the distortions from a 1-foot square simulated leak in 6.5 feet of water.

the effects are a linear function of depth. That is, as depth increases, a one-foot leak signature will result in equipotential plots similar to a one-inch leak signature at shallower depths. A discussion of this subject appears in the previous section.

An experiment was conducted to observe the influence of highly conductive metal objects close to a leak. Tests made with the physical scale model indicated no measurable influence of an aluminum block on leak signatures. To assess this effect, a 0.1-ft^2 simulated leak was positioned on the 90° radial, 60 feet from the current electrode. Measurements were made on the 60° to 120° radials. The raw data plot for the 90° radial is shown in Figure 48. These data established a baseline measurement without any metal objects. A peak occurs directly over the leak at the 60-foot odometer reading. Figure 49 shows the closing contours around the leak.

To assess the effects of metal objects, six 2-gallon metal cans were placed around the 0.1-ft^2 simulated leak in a circular pattern. Each can was positioned approximately 9 inches from the leak. Measurements were retaken under these conditions. A plot of the raw data along the 90° radial is shown in Figure 50. The shape of this curve is nearly identical to the shape of the 90° radial curve in Figure 48 for the test without cans. The only noticeable difference is that the magnitudes of the surface potential voltages are slightly lower with the cans. The contour plot of the can data presented in Figure 51 is nearly identical to the plot without the cans. It can be concluded from these results that the cans had a slight influence on the magnitude of the measurements, but did not change the signature of the 0.1-ft^2 leak to any great extent.

SEAM LEAK SIMULATION RESULTS

Geomembrane liners are typically joined at seams using various methods. An experiment was set up to determine the leak signature of a simulated seam leak 30 feet in length. An uninsulated copper wire was connected between two permanent leak locations in the pond. The ends of the wire were pushed through each leak cover and grounded using 12-inch steel stakes. The only metal surface exposed to the water was the wire. The surface area of the wire was calculated to equal 0.4 ft^2. The wire was located along the 90° radial, starting at 110 feet and ending at 140 feet away from the current electrode.

The raw data plot for the 90° radial is shown in Figure 52. The shape of the curve is significantly different from the point leak curves. It is much broader and the voltage gradient in the simulated leak zone is much smaller. The equipotential contour plot in Figure 53 shows these differences in the shape of the contour lines. The wire influences the surface potentials on all radial lines. The contours converge in the immediate location of the wire. As expected, the leak signature of an elongated seam failure is spread out along the radial and influences the current distributions in a much more significant way than do point leaks of the same surface area. This test demonstrates that the leak detection technique is sensitive to different leak geometries. These results indicate that the technique has the potential to distinguish between point leaks and seam leaks. The threshold limits where a

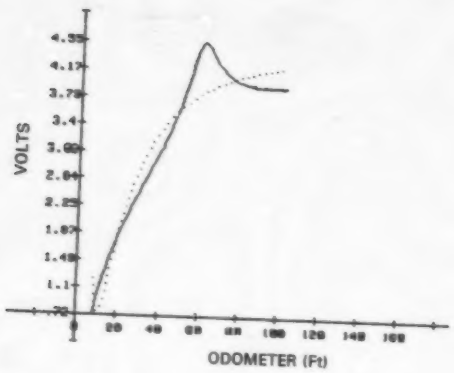

Figure 48. A plot of the potential measurements taken along the 90° radial. The peak occurs over a 0.1-foot square simulated leak without metal cans.

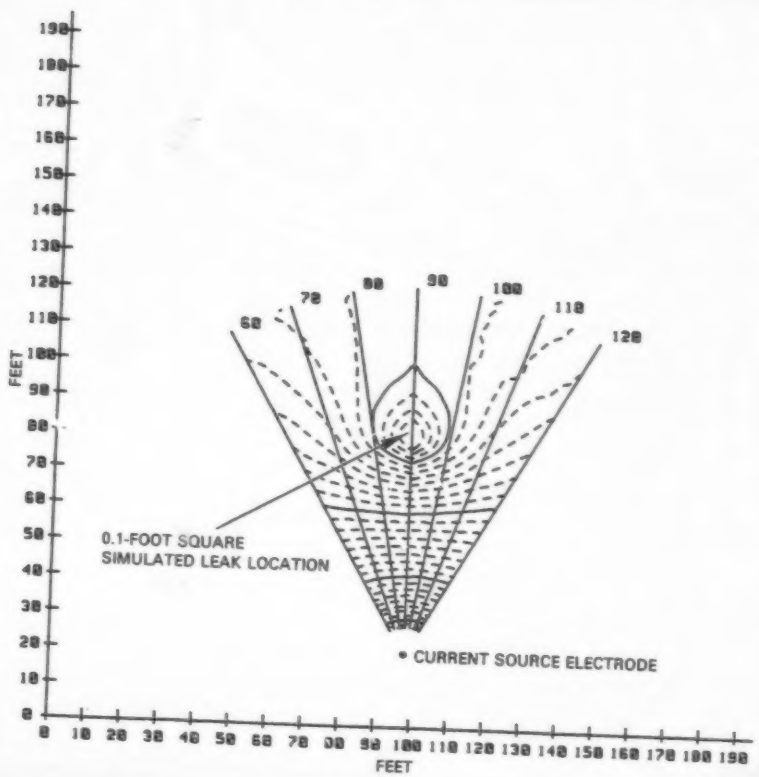

Figure 49. An equipotential contour plot showing the distortions from a 0.1-foot square simulated leak without metal cans.

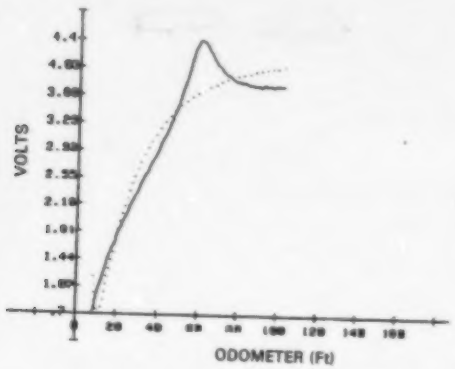

Figure 50. A plot of the potential measurements taken along the 90° radial. The peak occurs over a 0.1-foot square simulated leak with metal cans surrounding the leak.

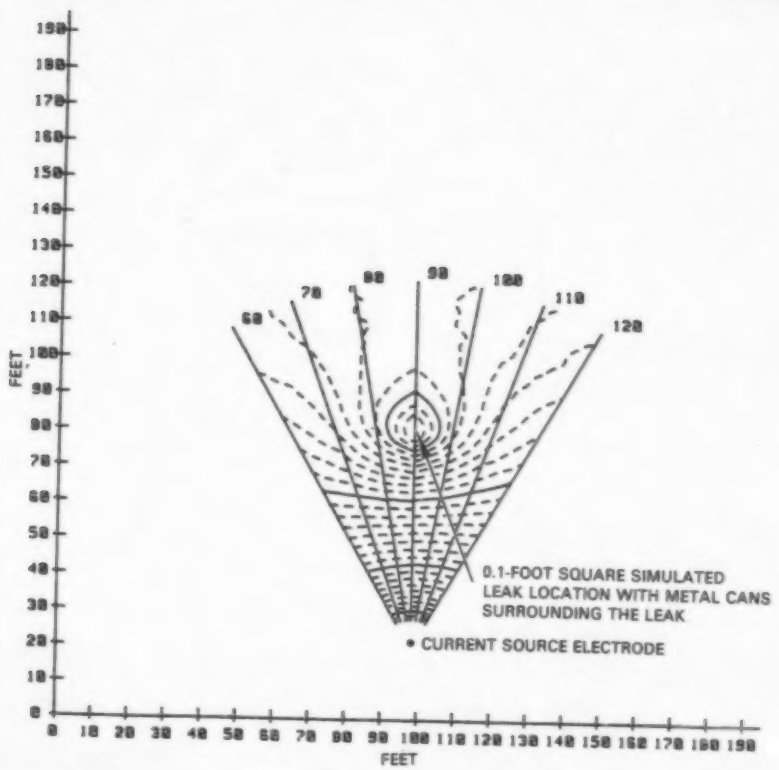

Figure 51. An equipotential contour plot showing the distortions from a 0.1-foot square simulated leak with metal cans surrounding the leak.

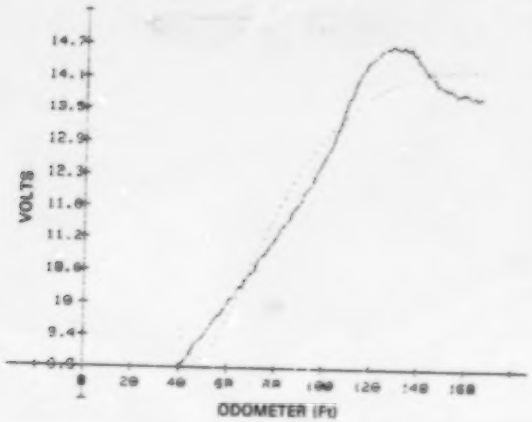

Figure 52. A plot of the potential measurements taken along the 90° radial. The peak occurs over a 0.4-foot square, 30-foot long wire used to simulate a seam leak.

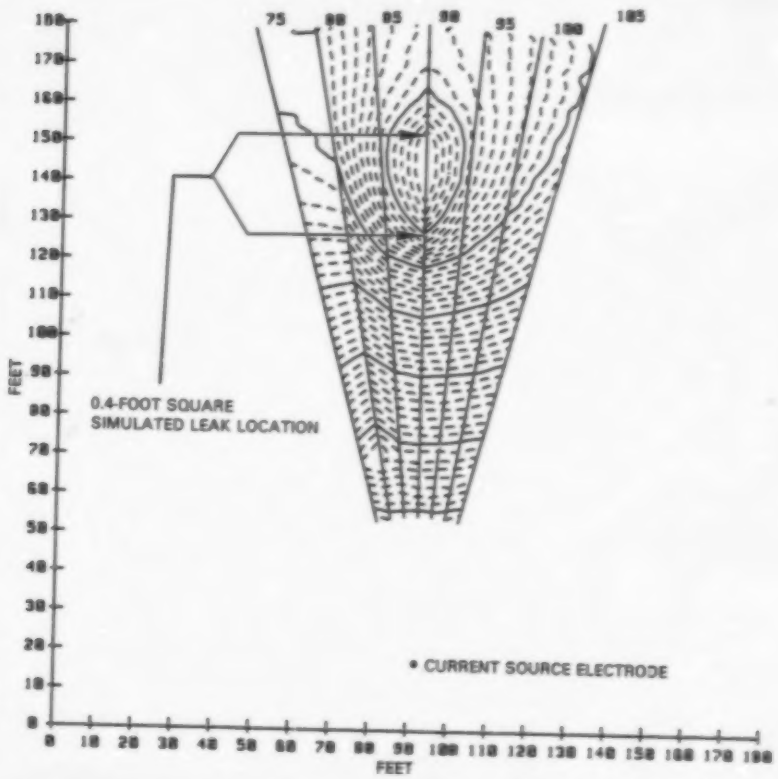

Figure 53. An equipotential contour plot showing the distortions from a 0.4-foot square, 30-foot long wire used to simulate a seam leak.

seam leak can be detected will, as demonstrated with the circular leaks, depend on surface area of the leak and depth of water over the liner.

MULTIPLE LEAK SURVEY RESULTS

Multiple leak configuration experiments were performed to determine the leak signatures and sensitivity of the electrical resistivity technique. For the first experiment, one-inch diameter leaks were installed at leak locations 01 and 04. Leak 01 is 72.3 feet away from the current electrode along the 90° radial. Leak 04 is 118 feet away from the current electrode along the 110° radial. Measurements of the surface potentials were made along the 60° to 140° radials from the water line back to 6 feet from the current electrode.

Figure 54 shows the raw data plots for the 90° and 110° radials. As with the single leaks, peaks of the measured data occur over the leaks. These peaks are, however, less pronounced than the corresponding peaks for the single leak configuration. Nevertheless, they are sufficient in magnitude to distort the equipotential contour lines in the area of each leak, as shown in Figure 55. The equipotential contour lines clearly show the presence of the two leaks. The plots in Figure 54 can be used to establish their locations to within one foot.

Another experiment was performed in which three one-foot diameter leaks were detected and located. These leaks were established at locations 01, 04, and 05. Surface potential measurements were at one-foot increments along the 70° through 125° radial lines. Figure 56 shows plots of the measured data along the 90°, 110° and 115° radials. Voltage peaks occur directly over each of the three leaks. The equipotential contour plot shown in Figure 57 clearly shows the presence of each leak.

A second experiment was conducted to determine the leak signatures of three different sized leaks located along the 90° radial. One-foot, 5-inch, and one-inch diameter leaks were established at leak locations 01, 02, and 03, respectively. Measurements were taken at one-foot increments along radial lines 75° through 105°. A plot of the measured data along the 90° radial is shown in Figure 58. The plot shows two large potential peaks at 70 ft and 110 ft and a small peak at 140 ft. The first two peaks correspond to the one-foot and 5-inch diameter leaks. The influence of the third one-inch diameter leak is very slight in terms of showing a perturbation in the curve. The roughness of these plots indicates noise in the data. Under these conditions, it would not be reasonable to predict that a leak existed at the 03 location based on the 90° plot of measured data in Figure 58. It appears that the effect of the first two leaks was to "mask" or "diminish" the effect of the third leak on the surface measurements.

The equipotential contour plot shown in Figure 59 clearly indicates the presence of the first two leaks. The shape of the contour line around the small one-inch diameter leak suggests that the leak did have an effect on the measurements which was not easily identified from examination of the raw data plots. If the presence of the leak at 03 had not been known, this plot would have been sufficient justification to resurvey the pond using a different electrode position. By repositioning the current injection electrode at a

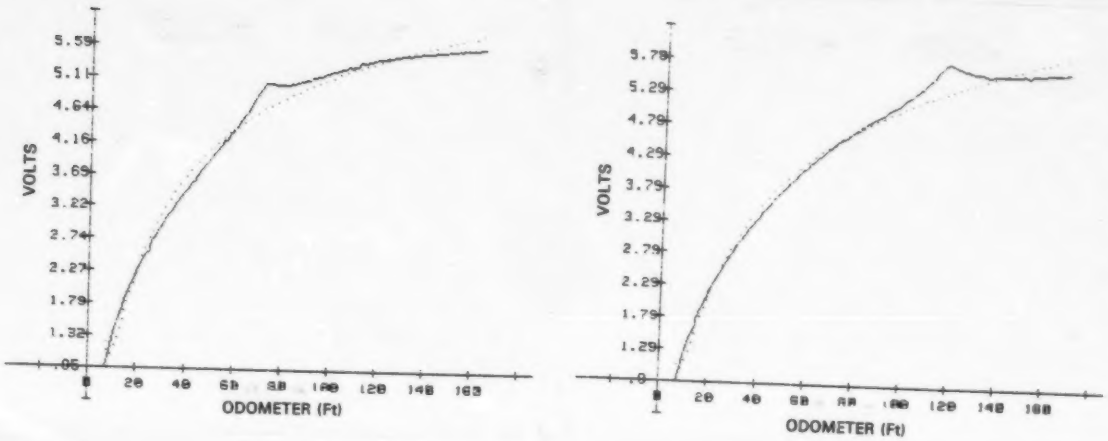

Figure 54. Plots of measurements along the 90° and 110° radials. Peaks occur over 1-inch diameter leaks.

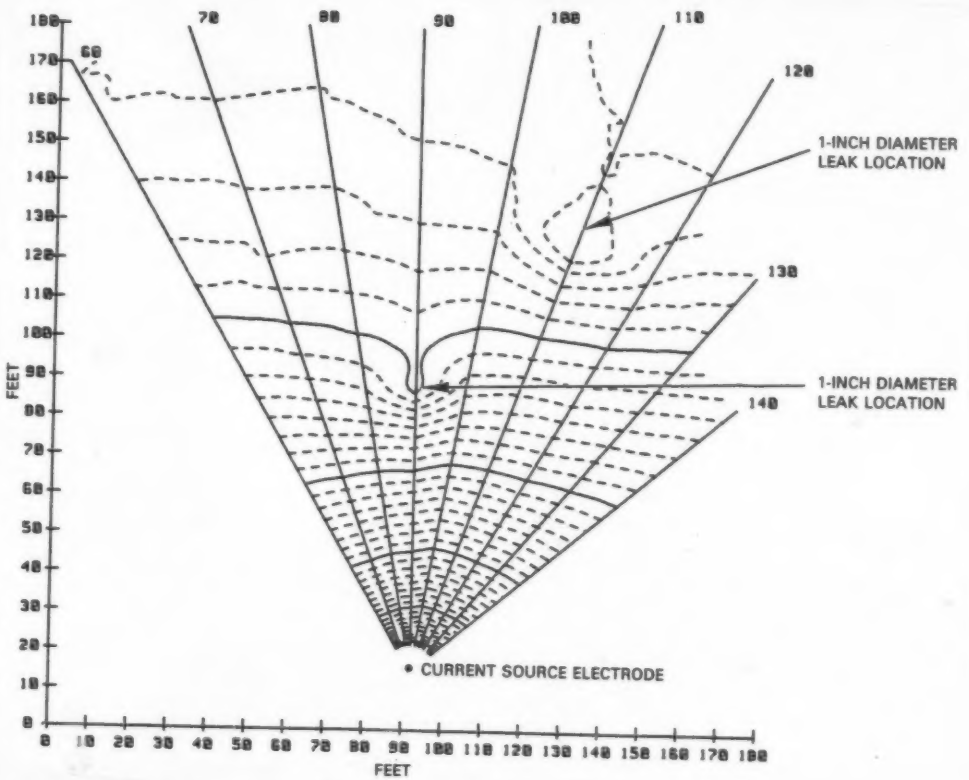

Figure 55. An equipotential contour plot showing the distortions from two 1-inch diameter leaks on two different radials.

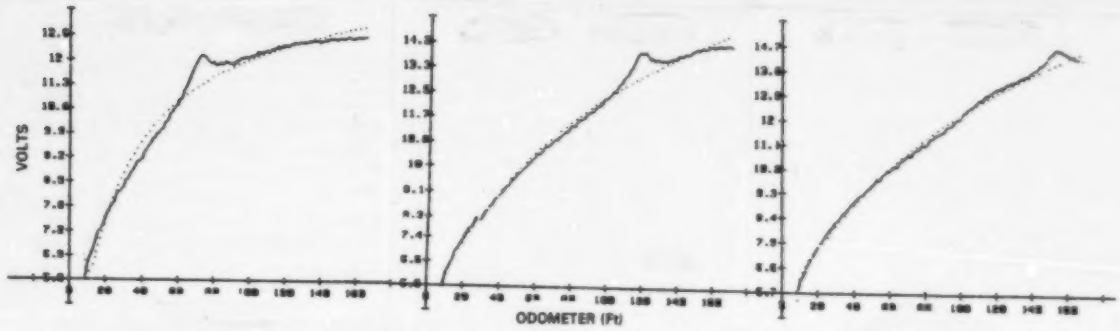

Figure 56. Plots of measurements along the 90°, 110° and 115° radials. Peaks occur over 1-foot diameter leaks.

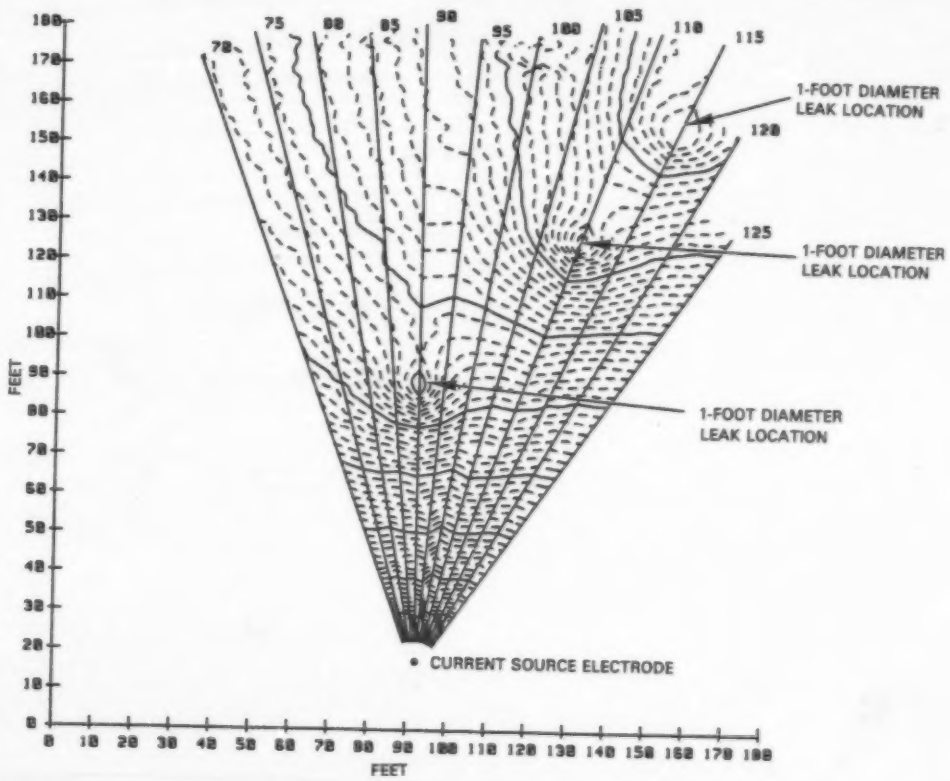

Figure 57. An equipotential contour plot showing the distortions from three 1-foot diameter leaks on three different radials.

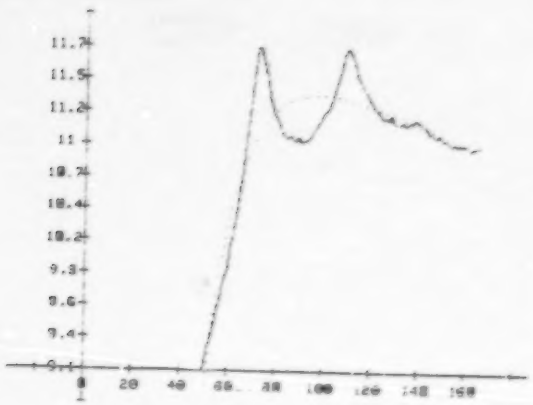

Figure 58. A plot of measurements along the 90° radial. Peaks occur over three different sized leaks.

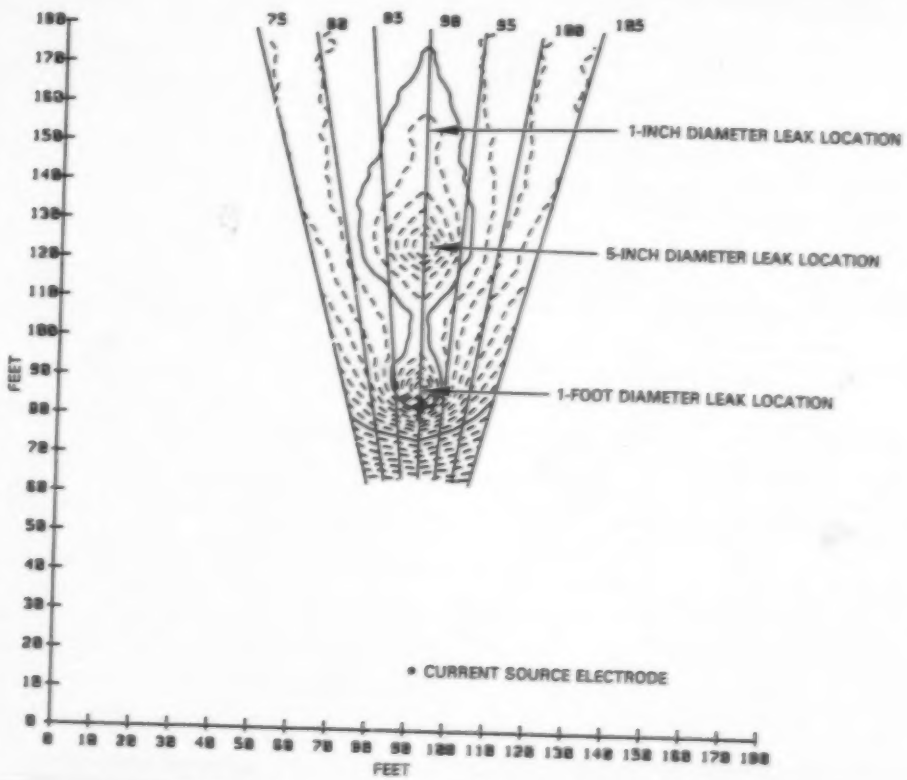

Figure 59. An equipotential contour plot showing the distortions from three different sized leaks along the 90° radial.

right angle to the 90° radial and moving closer to the leak location, the presence of the leak could possibly have been confirmed.

SUMMARY OF LARGE-SCALE TESTING

The results of the large-scale testing indicate single and multiple leaks in a geomembrane liner as small as one inch in diameter can be detected and located with an accuracy of one foot or less. This was achieved for leaks located in excess of 150 feet away from the current source electrode. The location of the leak does not appear to influence its detection or location to any significant extent. Increasing depth reduces the magnitude of the effects that a leak has on surface measurements. However, leak detection and location were not adversely affected. Depth of fluid over a liner system will influence leak detection and location. Measurements obtained for a one-inch diameter leak in 5 feet of water are predicted to be similar to measurements obtained for a 5-inch diameter leak in 25 feet of water. Future testing of the technique as well as improved computer modeling will further verify the validity of this prediction.

Metal cans positioned around a leak influenced the magnitudes of the measurements taken on the water surface over the leak. However, they did not prevent detection or location of the leak. Therefore, metal objects in lined surface impoundments are not expected to prevent detection or location of leaks.

Results of simulated seam leak tests suggest that the geometry of a leak can be determined from analyses of equipotential plots. The seam leak, simulated with a wire, elongates equipotential contour lines. The typical bull's-eye pattern produced by single point leaks is stretched along the length of the wire. Knowledge of this characteristic will be helpful when interpreting the results of surveys at other lined facilities.

REFERENCES

Hanrahan, D. 1979. Hazardous Wastes: Current Problems and Near-Term Solutions. Technol. Rev. 82(2):20-31.

EPA. 1980. Research Outlook 1980. EPA 600/9-80-006. U.S. Environmental Protection Agency, Washington, DC. 224 pp.

Surface Impundment Assement National Report. U.S. Environmental Protection Agency, Office of Water, Office of Drinking Water. December, 1983. 154 pp.